VOLUME 18, 1956/57, No. 9 pp. 249-284 Published 10th February 1957

Philips Technical Review

DEALING WITH TECHNICAL PROBLEMS
RELATING TO THE PRODUCTS, PROCESSES AND INVESTIGATIONS OF
THE PHILIPS INDUSTRIES

EDITED BY THE RESEARCH LABORATORY OF N.V. PHILIPS' GLOEILAMPENFABRIEKEN, EINDHOVEN, NETHERLANDS

COLOUR AND COLOUR RENDERING OF TUBULAR FLUORESCENT LAMPS

by A. A. KRUITHOF and J. L. OUWELTJES. 621.327.534.15:535.625

The tubular fluorescent lamp has given rise to all kinds of new problems in lighting technology which were irrelevant or insoluble in the case of the incandescent lamp. Illumination by distributed light sources (as opposed to point sources) required new investigations; the design of fittings again raised the question as to permissible brightnesses; the high luminous efficiencies and the white colour of the light from the first fluorescent lamps led to reconsideration of desirable levels of illumination; the fact that it was possible to vary the spectral distribution of the light from the lamps within wide limits, led to investigations regarding the most desirable colour for the light and discrepancies in the colour rendering. This article describes how the latter investigations have resulted in a range of lamps with a largely natural colour rendering.

The colour of tubular fluorescent lamps

It was about 25 years ago that the first attempts were made to coat the wall of the low-pressure mercury-vapour lamp with a fluorescent powder (phosphor) and in this way to arrive at a lamp for general lighting purposes. The phosphor converts the ultra-violet radiation from the low-pressure mercury-vapour discharge, especially the spectrum line of wavelength 2537 Å, into visible light. This conversion can be brought about with high yield, so that the resulting lamp may have a very high luminous efficiency, much higher than that of the incandescent lamp. High luminous efficiency is one of the chief features of the modern tubular fluorescent lamp, which is the fruit of those early efforts.

The search for suitable fluorescent substances was soon so successful that it became possible by using a mixture of phosphors in the fluorescent coating to produce light in a wide variety of colours. The question then arose as to exactly what colour was desirable.

Initially the only guiding principle was that lamps for general lighting purposes should give an impression of "whiteness". Closer study reveals that "white" is a far from well-defined colour. The human eye is willing to see a white tablecloth as "white" both by daylight and by incandescent-lamp light, and, indeed, even by candlelight, despite the fact that the radiation it receives from the cloth is totally different in each case. This is known as "chromatic adaptation" of the eye [1]).

The differences between the radiations from the above-mentioned sources are only apparent to the eye if they are present in the visual field at one and the same time. Now this state of affairs was frequently encountered in fluorescent-lighting practice. For example, fluorescent lamps had to be used for supplementary day-time lighting in dark shops and offices, or in combination with incandescent lighting which was already present, or was required for special effects. When colour differences were too great, false effects and coloured shadows resulted — troublesome phenomena which had already been met with, of course, in combining incandescent-lamp light with daylight. They had then been accepted as unavoidable in most cases. With fluorescent lamps, where the choice of fluorescent substances offered greater freedom, there was no need to accept these troublesome phenomena. Hence the vague guiding principle, already referred to, was subsequently narrowed down to state that the colour

[1]) A. A. Kruithof and P. J. Bouma, Physica **9**, 957-966, 1942; P. J. Bouma and A. A. Kruithof, Physica **10**, 36-46, 1943. See also Philips tech. Rev. **9**, 2-7 and 257-266, 1947/48.

of the fluorescent light must resemble that of daylight or that of incandescent-lamp light. A complication that now arises is that "daylight" can vary continuously within wide limits according to the height of the sun and to the weather conditions. The colour of incandescent-lamp light can also vary somewhat according to the temperature of the filament. In order to fix the desired colour more exactly, use is made of the fact that most variants of daylight, as well as incandescent-lamp light, closely resemble the radiation emitted by a black body at a certain temperature. Hence these sources can be characterized by the corresponding temperature of the black body (colour temperature). *Table I* gives the colour temperatures for a number of light sources.

Table I. Colour temperatures for a number of light sources.

Light source	Colour temperature in °K
Blue sky	10000-20000
Overcast sky	5000-7500
Direct sunlight (midday)	approx. 5000
Carbon arc	approx. 3750
Photoflood lamp	approx. 3200
Incandescent lamp	2400-3000
Candle	1900

In addition to fluorescent lamps for combination with daylight and others for combination with incandescent lamps, lamps which might be used with both types of light were considered. Naturally such lamps involve a compromise. In order to explain the choice of the colour for such a lamp, we must make use of the well-known representation of colours by points in a chromaticity diagram [2]); see *fig. 1*. The points for the incandescent black body at various temperatures lie on a certain curve in the figure — the black-body locus — and on or very near this curve will be situated the points for the selected types of "daylight" (D) and "incandescent-lamp light" (G). An obvious choice for the compromise would be the colour point which lies halfway along the line connecting D and G. However, the colour contrasts with respect to D and G are found to be somewhat less troublesome for a colour which is situated on (or very close to) the black-body locus and whose colour temperature is nearer that of G than that of D.

Another consideration in designing a lamp with its colour point between D and G, was that the colour Daylight was only found to be agreeable at relatively high levels of illumination — even when the lamp was not used in combination with natural daylight. This point has been discussed at length in an earlier article in this journal [3]).

Thus by a process of trial and error, three standard types of fluorescent lamps have been arrived at, which conform to the practical requirements and have the following colour temperatures and colour points [4]):

a) "Cool Daylight", 6800 °K, with trichromatic coefficients (coordinates in the chromaticity diagram) $x = 0.308$, $y = 0.324$ (see fig. 1). (This lamp has no equivalent in England, but corresponds to the "Daylight" lamps of American manufacturers.) Lamps of this type are suited for use in combination with average daylight.

b) "Warm White", 2900 °K, trichromatic coefficients $x = 0.440$, $y = 0.399$. These lamps are suitable for use alongside incandescent lamps; their light is only slightly bluer than that of the larger incandescent lamps (colour temperature between 2600 and 2850 °K).

c) "White", 4200 °K, trichromatic coefficients $x = 0.371$, $y = 0.368$. If necessary, these lamps can be combined both with daylight and with incandescent lamps. (This Dutch lamp corresponds to the English "Daylight" lamp ($T_c = 4500$ °K) and to the American "Cool White" ($T_c = 4400$ °K).)

In order to be able to make these lamps, it is necessary to have available phosphors which give sufficient latitude to allow the desired colour points to be realized. How great this latitude is with three current phosphors can easily be seen if the colour points of these phosphors are indicated in the chromaticity diagram. In fig. 1, the colour points are shown for three phosphors which are suitable for use in fluorescent lamps, viz. calcium silicate, activated with lead and manganese; calcium tungstate; and zinc silicate activated with manganese (willemite). Any colour point within the triangle formed by these three points can be obtained by mixing the three phosphors mentioned in the correct proportions. Nowadays halophosphates are often used for the fluorescent coating. With these materials there is a certain amount of colour mixing in the phosphor itself [5]): halophosphates have two

[2]) See in this connection P. J. Bouma, Philips tech. Rev. **1**, 283-287, 1936, and **2**, 39-46, 1937; a more comprehensive exposition is to be found in the book by the same author: Physical aspects of colour, Philips Technical Library, 1946.

[3]) Philips tech. Rev. **6**, 69, 1941, fig. 10.

[4]) Attempts are also being made to gain international acceptance of three standard colours, whose colour points differ only slightly from those reported here.

[5]) J. L. Ouweltjes, New phosphors for fluorescent lamps, Philips tech. Rev. **13**, 346-351, 1951/52.

emission bands, one in the blue (at about 4800 Å) and one in the orange (at about 5900 Å). The location of the latter band and the ratio between the intensities of the two bands can be varied somewhat by varying the composition of the halophosphate, so that here also a diagram of colour points, albeit a narrow one, can be obtained.

One important advantage of the halophosphates is that the colour points of the lamps are more readily reproducible in mass production. Also, small deviations from the correct composition give rise to a displacement of the colour point approximately along the black-body locus. Such a displacement is far less troublesome than a displacement at right angles to this line.

To conclude this introduction we shall describe briefly how the proportions are calculated in which three given phosphors (or, rather, their light contributions) must be mixed in order to produce a lamp with a predetermined colour point (x, y). The formulae used in this calculation form the basis of all the calculations which will be discussed later in this article.

The formulae are simplest if we introduce the trichromatic coordinates (coordinates in the three-dimensional colour space) of the colour points of the phosphors: X_1, Y_1, Z_1; X_2, Y_2, Z_2; X_3, Y_3, Z_3 [6]). Each trichromatic coordinate of the colour of a

[6]) For fuller details regarding the coordinates X, Y, Z in colour space and the trichromatic coefficients x, y which fix the location of a point in the chromaticity diagram, see for example the book cited in [2]), pp. 73 et seq. and 80 et seq.

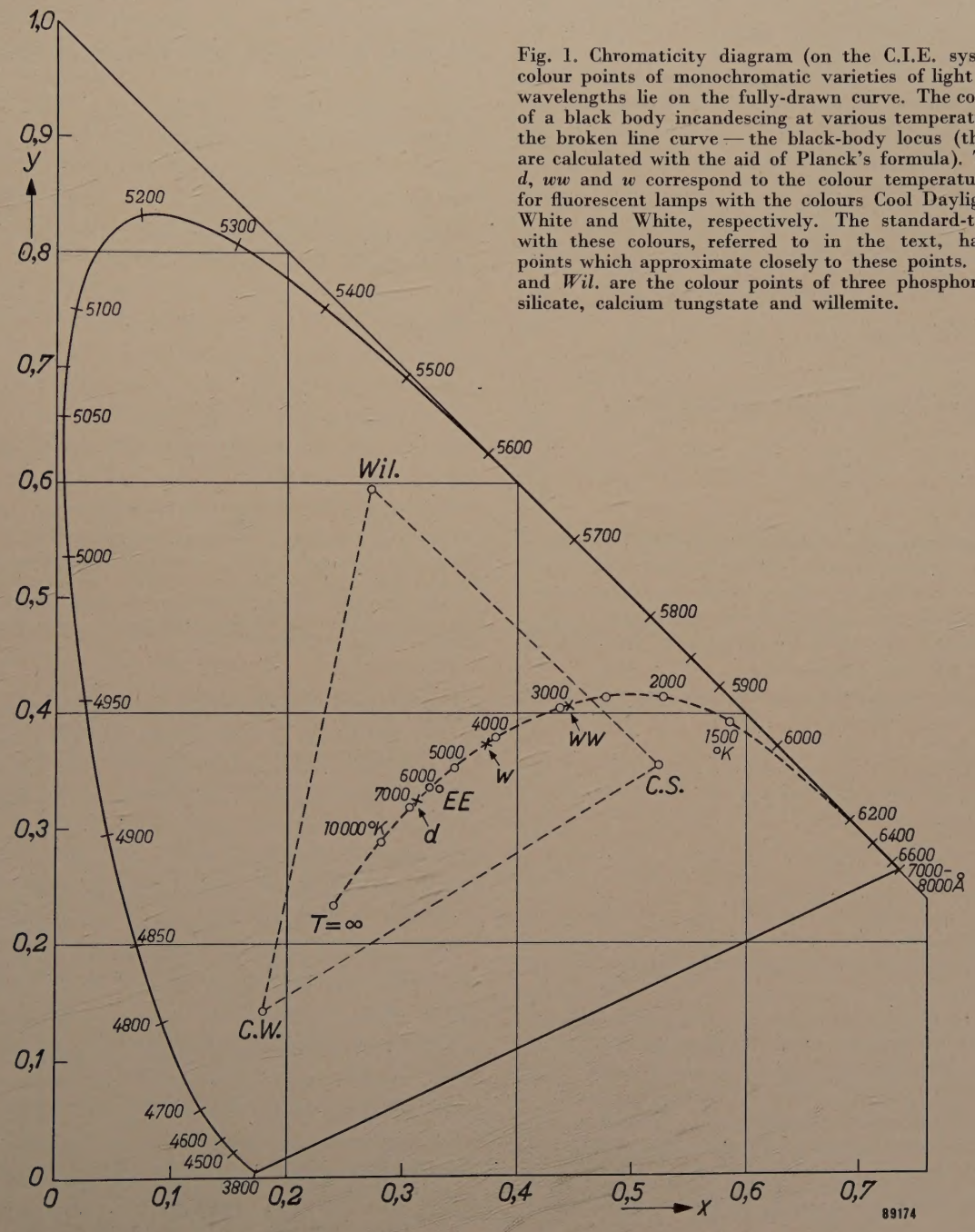

Fig. 1. Chromaticity diagram (on the C.I.E. system). The colour points of monochromatic varieties of light of various wavelengths lie on the fully-drawn curve. The colour points of a black body incandescing at various temperatures lie on the broken line curve — the black-body locus (these points are calculated with the aid of Planck's formula). The points *d*, *ww* and *w* correspond to the colour temperatures chosen for fluorescent lamps with the colours Cool Daylight, Warm White and White, respectively. The standard-type lamps with these colours, referred to in the text, have colour points which approximate closely to these points. *C.S.*, *C.W.* and *Wil.* are the colour points of three phosphors: calcium silicate, calcium tungstate and willemite.

mixture is the sum of the respective coordinates of the components, each multiplied by a factor (α, β, γ) which determines the mixing proportion. The coordinates Y_1, Y_2, Y_3 indicate the value of the luminous flux which each of the phosphors would supply in a 40-watt lamp containing that phosphor only (all calculations are based on a constant lamp power, viz. 40 W). In a 40-watt lamp the mixture then gives a luminous flux of $\alpha Y_1 + \beta Y_2 + \gamma Y_3$. The luminous fluxes Y_1, Y_2, Y_3 are of course different, since the phosphors convert the absorbed ultra-violet quanta into quanta to which the human eye is sensitive to varying degrees. The "quantum yield", i.e. the number of visible quanta emitted divided by the number of ultra-violet quanta absorbed, is almost the same for all phosphors in practical use, being about 90%; hereafter we shall assume that it is always exactly the same.

Apart from fluorescent light, a fluorescent lamp always emits a certain amount of visible light that originates directly from the mercury vapour discharge; this contribution to the luminous flux is absorbed hardly at all by the normal fluorescent layer and depends therefore only on the given power of the lamp and not on the nature of the phosphors or the proportions in which they are mixed. The trichromatic coordinates of the colour point for this mercury light we shall call X_{Hg}, Y_{Hg}, Z_{Hg}, those of the light from the resulting lamp X, Y, Z. We then have:

$$\left.\begin{aligned} X &= \alpha X_1 + \beta X_2 + \gamma X_3 + X_{Hg}, \\ Y &= \alpha Y_1 + \beta Y_2 + \gamma Y_3 + Y_{Hg}, \\ Z &= \alpha Z_1 + \beta Z_2 + \gamma Z_3 + Z_{Hg}. \end{aligned}\right\} \quad \ldots \quad (1)$$

The factors α, β, γ must satisfy the condition

$$\alpha + \beta + \gamma = 1, \quad \ldots \ldots \ldots \quad (2)$$

since the quantum yield is the same for all the phosphors and the total number of quanta available to the phosphors for conversion is constant for a given discharge wattage (i.e. it is independent of the composition of the fluorescent coating); increase of any one contribution therefore is always at the expense of the other contributions.

Further, for the desired lamp the following trichromatic coefficients [6]) are stipulated:

$$\left.\begin{aligned} x &= \frac{X}{X+Y+Z}, \\ y &= \frac{Y}{X+Y+Z}. \end{aligned}\right\} \quad \ldots \ldots \quad (3)$$

(The reason why it is impossible to stipulate the three trichromatic coordinates of the lamp is connected with the fact that the total luminous flux of the lamp for a given power cannot be predicted, since the resultant luminous efficiency of the phosphor mixture is for the time being unknown.) The six quantities α, β, γ, X, Y, Z are determined by the six equations (1), (2) and (3). Thus the required proportions in which the phosphors must be mixed can be calculated. If the stipulated colour point lies within the above-mentioned triangle of the colour points of the phosphors, positive values are always found for α, β, γ, i.e. the colour can be realized.

Colour rendering

Thus far we have only discussed colour points, but have ignored the fact that sources with quite different spectral energy distributions may have the same colour point. This is illustrated by *fig. 2*. Radiation *a* with a so-called equal energy spectrum (the energy in a narrow wavelength range $\Delta\lambda$ is the same at all wavelengths) appears "white" and has the colour point $x = {}^1/_3$, $y = {}^1/_3$ (*EE* in fig. 1). Radiation *b* comprising only the wavelengths $\lambda =$ 5890 Å and $\lambda = 4860$ Å, the latter having twice the energy of the former (both for the sake of clarity broadened out in the figure into a wavelength range of 200 Å), has the same colour point and hence gives the same impression of whiteness. The colours of objects, however, are in general rendered quite differently by the two types of light. A red object,

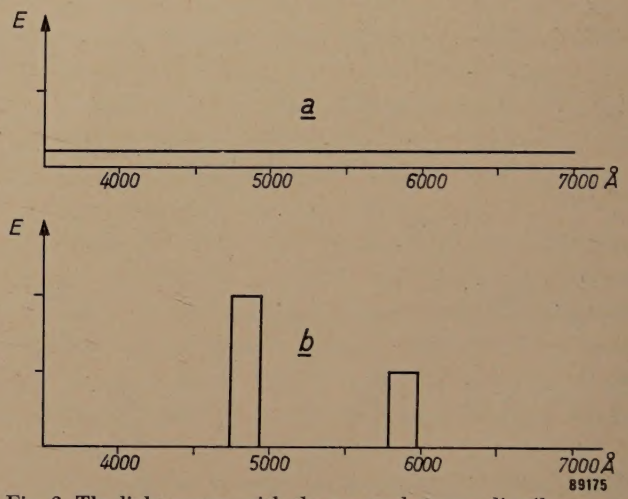

Fig. 2. The light source with the spectral energy distribution *a* (equal energy spectrum) has the identical white colour of and the same luminous flux as that with the spectral distribution *b*. The colour point of both light sources in the chromaticity diagram in fig. 1 is *EE* ($x = {}^1/_3$, $y = {}^1/_3$).

reflecting only the red rays of the light falling upon it, will appear black or dark brown by light *b*. By light *a* it will have its natural colour, and this will be the case not only for red objects but for objects of any colour. In light *b* only yellow and blue objects will retain approximately their natural colours. The colour rendering of *b* is therefore poor, that of *a*, on the other hand, very good or "natural".

Owing to the chromatic adaptation of the human eye, there are quite a number of types of light in which almost all objects give us the impression of having their natural colours, in spite of differences in the spectral energy distributions of these types of light and the resulting differences in the colour coordinates for the same given object. Notable examples of such types of light are daylight in all its varieties, incandescent-lamp light and,

we may assume, the radiation from black bodies at intermediate temperatures. For these reasons (and also because they are found naturally) all thermal radiators are called "natural light sources".

Returning to fluorescent lamps, the above discussion shows that the mere establishment of the colour points for the three standard lamps in no way establishes the spectral energy distribution for each of these lamps. The latitude which still remains, and which therefore permits of choosing phosphors with a great diversity of spectral distributions as the components of the mixture, can be made use of to achieve two different ends:

1) to give the lamps the highest attainable luminous efficiency [7]);
2) to make the colour rendering of the lamps as good as possible.

In the above-mentioned standard-type lamps, high luminous efficiency is given first consideration; for the Cool Daylight lamp, a luminous efficiency of 55 lumens per watt has been attained, for the Warm White lamp 67.5 lm/W and for the White lamp 61 lm/W. (Incandescent lamps for general lighting give 20 lm/W at most.) In addition the past few years have witnessed intensive work on fluorescent lamps in which the emphasis has been in the other direction — on the colour rendering qualities. The colour points of such lamps should be practically the same as before. In what follows we shall see how the task of improving the colour rendering has been set about and what results have been obtained in regard to these so-called "de Luxe" lamps.

It is first necessary to show in which respects the colour rendering of the standard fluorescent lamps falls short. This can be done by comparing the spectral distribution of these lamps with that of natural light sources, i.e. black bodies with corresponding colour temperatures. This comparison is made in *fig. 3a-c* for the energy distributions and in *Table II* for the light flux, employing a subdivision of the spectrum into the eight wavelength bands introduced by Bouma [8]). Further, there must be some means of assessing how badly the differences in the spectral distributions of the lamps affect their colour rendering qualities. A means of assessment which was found empirically is Harrison's figure of merit. The figures of merit are calculated from the eight-band light-flux distribution[9]) and have been included in the table. A more direct, though more laborious method consists in directly

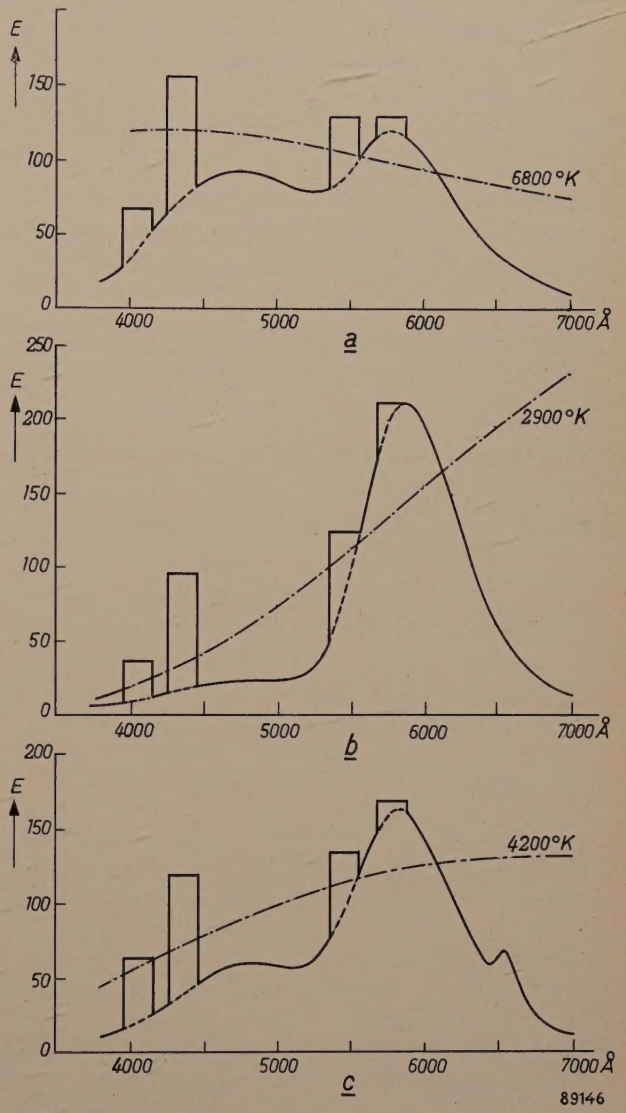

Fig. 3. The spectral energy distributions of the standard types of 40-watt fluorescent lamps (halophosphate phosphors).
a) Lamp colour "Cool Daylight", colour temperature 6800 °K, luminous flux 2200 lm.
b) "Warm White", 2900 °K, 2700 lm.
c) "White", 4200 °K, 2450 lm.
The energy scale for the fluorescent lamps is the same in all three figures. The broken line in each figure represents the spectral distribution of the corresponding black body, the scale being such that the luminous flux is the same as that of the lamp in question.

[7]) It will be clear that a high luminous efficiency is attainable if the spectral distribution of the components favours those spectral bands to which the eye is most sensitive. The halophosphates are especially rich in emissions of these wavelengths.

[8]) P. J. Bouma, Philips tech. Rev. **2**, 1-7, 1937. Later the subdivisioning was changed somewhat, so that the spectral bands shown in the table are now used. In 1948 this method of assessing colour rendering was recommended by the C.I.E. (Commission Internationale de l'Eclairage).

[9]) Let l_i be the relative luminous-flux contribution of the lamp in the i^{th} spectral band, z_i that for the corresponding black body and E_i that for the radiator with an equal energy spectrum (fig. 2*a*). Harrison now calculates the ratios l_3/l_6, l_4/l_6, l_5/l_6 and $(l_7+l_8)/l_6$ and divides these by the corresponding ratios E_3/E_6 etc. The average difference between the calculated ratios and the corresponding ratios for the black body (i.e. $z_3/z_6 : E_3/E_6$ etc.) is multiplied by 100; subtracting the result from 100 gives Harrison's "figure of merit". See W. Harrison, Light and Lighting **44**, 148-153, 1951.

comparing the colours of a series of objects in both kinds of light, either experimentally or by calculation. In the calculation the colour points of the test objects are determined when lighted with the two sorts of light to be compared, starting from the given spectral reflection curves (reflection coefficient as a function of the wavelength). Since the two sorts of light being compared have the same colour point (only their spectral energy distributions differ), the state of chromatic adaptation of the eye is the same, so that identity of colour point also signifies identity of colour sensation. Judd [10]) has constructed a chromaticity diagram (the Uniform Chromaticity Scale or UCS diagram) in which, given that the chromatic adaptation of the eye is constant, the distance between two colour points is approximately proportional to the difference in colour which is observed. A distance of 0.01 is clearly observable as a difference in colour. In the calculations for 15 coloured objects, some with saturated and some with unsaturated colours (one of the latter corresponding to the colour of the skin), the greatest colour discrepancy Δ_m of the Cool Daylight lamp, compared with the black body at corresponding temperature, was found to be 0.045, that of the Warm White lamp 0.065 and that of the White lamp 0.05.

Table II. Relative spectral light-flux distributions of the standard fluorescent lamps and their corresponding black bodies. The spectrum is divided into eight bands after Bouma. Harrison's figure of merit H is also given for each kind of light.

Spectral band		"Cool Daylight"		"Warm White"		"White"	
No.	Wavelengths in Å	Fluorescent lamp	6800 °K	Fluorescent lamp	2900 °K	Fluorescent lamp	4200 °K
I	3800-4200	0.017	0.037	0.006	0.006	0.010	0.017
II	4200-4400	0.44	0.27	0.28	0.062	0.33	0.14
III	4400-4600	0.66	0.86	0.15	0.26	0.33	0.50
IV	4600-5100	8.9	10.9	2.3	5.5	5.1	8.1
V	5100-5600	41.8	42.0	29.2	33.7	35.7	38.6
VI	5600-6100	41.5	33.5	57.3	42.5	49.6	39.1
VII	6100-6600	6.5	9.7	10.5	16.4	8.8	12.5
VIII	6600-7800	0.15	0.67	0.21	1.54	0.21	0.99
Figure of merit H		67	100	62	100	64	100

The development of the "de Luxe" colours

In attempts to improve the colour rendering qualities, the spectral energy distributions of the lamps, as given in fig. 3, were taken as a guide. The most serious deficiencies from the ideal distribution (i.e. that of the corresponding black body) are:

1) deficiency in the extreme red spectral region (spectral band VIII);
2) the occurrence of two humps in the spectrum, one in the blue-violet (mercury line 4358 Å) and one in the yellow-green (about 5800 Å). The two humps are interrelated: to compensate for the unavoidable strong blue-violet mercury line special provision has to be made in formulating the phosphor mixtures, to obtain a hump in the complementary colour, the yellow-green [11]).

Qualitatively, it can readily be understood how the deviations from the ideal curve adversely affect the colour rendering. Owing to deficiency (1) (above) red colours are not faithfully reproduced: bright red colours assume a dull look. Deficiency (2) is particularly detrimental to the rendering of yellow and orange objects: the extra light contributions in the blue-violet and the yellow-green do, it is true, compensate each other on an object which reflects both kinds of radiation, e.g. a white cloth, but yellow and orange objects absorb the surplus blue-violet, so that the excess of yellow-green is no longer neutralized. The result is the familiar green discoloration which such objects assume when illuminated by standard fluorescent lamps. A notorious case is that of certain foodstuffs, such as butter, potatoes and fruit, which in this light often assume a somewhat unpalatable appearance. Similarly, blue-coloured objects are given a violet tinge, but this is usually found to be less troublesome.

Deficiency (1) is present in the same degree in all three types of fluorescent lamps (Cool Daylight, White, Warm White). Deficiency (2) demands more attention in the case of the Warm White and White lamps than in the case of the Cool Daylight lamp. This too is understandable. The contribution of the mercury light (and of the blue-violet mercury line, therefore) is pretty well independent of the colour of the lamp (see equation 1). In the Warm White and White lamps, which emit only a relatively small amount of blue radiation (figs. 3*b* and *c*), the latter is for the most part concentrated in the mercury line; in the Cool Daylight lamp for which the contribution of the continuous spectrum in the blue is much larger (fig. 3*a*), the contribution of the mercury line plays a less important role.

We shall now discuss in turn remedies that have been tried for both deficiencies.

[10]) D. B. Judd, J. Opt. Soc. Amer. **25**, 24-36, 1935.

[11]) The complementary colour of 4358 Å must be determined separately for each lamp by drawing a line from the point for that wavelength through the colour point of the lamp to the opposite side of the chromaticity diagram. With all three lamp colours discussed here we arrive at the yellow-green.

The admixing of red

Starting from the standard-type lamps with a halophosphate fluorescent layer attempts have been made to remedy the deficiency in the red by adding a new, red-fluorescing phosphor to the phosphor mixture. Magnesium arsenate [5]) with a strong emission band in the deep red (maximum at 6560 Å) was found to be a suitable phosphor. When this phosphor is added to the mixture, the colour point of the lamp shifts in the first instance to the right and to below. In order to restore the colour point to its former position, the blue emission band of the halophosphate must be made stronger (shift to the left) and at the same time a green phosphor, e.g. willemite, must be added to give the necessary return shift upwards.

If for the sake of simplicity we regard the two bands of the halophosphate (orange and blue) to be derived from separate phosphors, we are then dealing with a mixture of four components. Obviously the mixing proportions are not now unequivocally determined by the assigned colour point: any one of the proportions can be given an arbitrary value. Here we have chosen the ratio between the two reddest phosphors. If we call this ratio a, we can then put the following question: for which value of a does the colour rendering of our mixture least deviate from that of the black body that corresponds to the lamp?

To be able to answer this question, we have again calculated the colour points in Judd's UCS diagram, of the fifteen coloured objects already mentioned, for a series of mixtures with various values of the parameter a, viz. 0, 0.2, 0.4, 0.5, 0.6, 0.8 and 1. In *fig. 4* the calculated colour points L_p for five of the objects are indicated for $a = 0$, $a = 0.5$ and $a = 1$, for the lamp colour "White", which corresponds to that of a black body radiating at 4200 °K. The colour points N_p of the objects when illuminated with this black body are likewise given. The distance Δ_p from L_p to N_p has been calculated for the above values of a and is plotted in *fig. 5* as a function of a [12]) for all 15 objects ($p = 1$ to 15).

Although the minima of Δ_p do not occur for the same value of a for all the coloured objects, it can

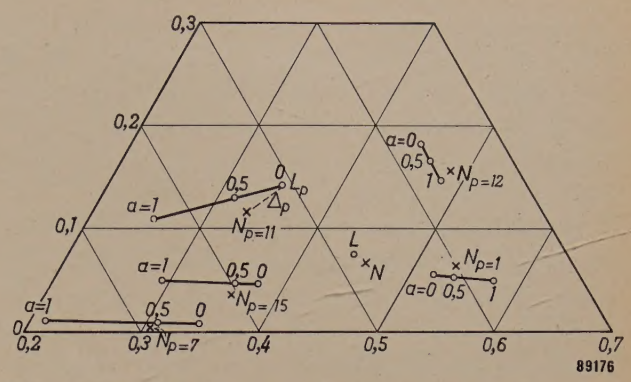

Fig. 4. Part of the Uniform Chromaticity Scale diagram after Judd [10]). This diagram — which is derived by linear transformation from the chromaticity diagram of fig. 1 (see for example the book by Bouma cited in [2])) — is such that equal distances correspond to equal differences in colour sensation (equal number of steps in which the colour difference is just perceptible).

The points N_p with p = 1-7-11-12-15 are the colour points of five test objects (coloured objects p, see fig. 5), illuminated by a black-body radiation at 4200 °K. At the same time, the colour points L_p are given for each object, these representing the colour it assumes when illuminated by means of a white fluorescent lamp with magnesium arsenate added to the phosphor, for various values of a, the proportion in which the two red phosphors are mixed. The colour points obtained by varying a always lie on straight lines. N is the colour point of the black body mentioned, L is that of the fluorescent lamp.

be seen from fig. 5 that for the lamp colour White, there is a region in the neighbourhood of $a = 0.5$ where most of the colour discrepancies Δ_p are markedly smaller than for higher or lower values of a.

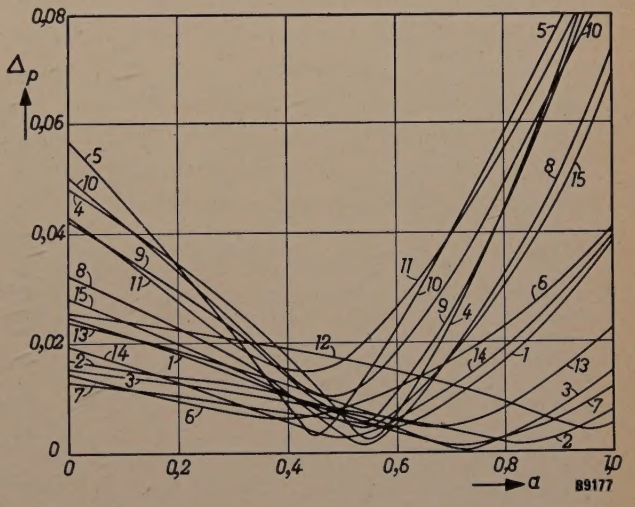

Fig. 5. Colour discrepancies Δ_p, represented as distances in the UCS triangle, for coloured objects with the numbers $p = 1$ to 15, illuminated by a black-body radiator at 4200 °K and then by a white fluorescent lamp with the mixing parameter a. For a specific value of a, in this case $a \approx 0.5$, the colour differences are at a minimum. The greatest remaining colour discrepancy Δ_m — in the case in point $\Delta_m \approx 0.017$ — indicates the best colour rendering that can be attained by adding magnesium arsenate.

The objects $p = 1$ to 6 are the pigments green, blue, yellow, orange, red and purple, whose spectral reflection curves are given in Hardy's Handbook of Colorimetry (M.I.T., Cambridge, Mass., 1936); $p = 7$ to 15 are the colours pa 04, pa 17, pa 25, pa 33, nc 42, nc 54, nc 71, pa 88 and ia 21 from Ostwald's Colour Atlas.

[12]) The mixing of the two red phosphors with colour coordinates X_1, Y_1, Z_1 and X_2, Y_2, Z_2 in the ratio a means that we are replacing the two phosphors by one phosphor with coordinates $aX_1+(1-a)X_2$, $aY_1+(1-a)Y_2$, $aZ_1+(1-a)Z_2$. The colour of an object L_p calculated for this mixture, however, can always be regarded as a mixture of the original colours as calculated for $a=0$ and for $a=1$. It follows from this that, on variation of a, each colour point L_p shifts along the straight line connecting the two extreme positions of L_p. This property makes it relatively easy to construct fig. 5 by interpolation.

The greatest remaining colour discrepancy for $a = 0.5$ is $\Delta_m = 0.017$. a will thus be chosen to lie in this region, and the other mixing-proportions of the phosphor mixture then follow from the desired colour point, which is selected to have the same value as that of the standard White lamp.

In narrowing down the choice of a, the desirability of having a high efficiency must be borne in mind. True, the efficiency is only a secondary consideration here, but it is one nevertheless which cannot be totally ignored: a relatively small reduction in Δ_m is not justified if it would mean a great sacrifice in luminous efficiency. Thus the White de Luxe lamp was developed with the phosphors mentioned and $a = 0.34$. The greatest colour discrepancy occurring with this lamp in the UCS triangle is $\Delta_m = 0.023$, the Harrison figure of merit is 76.

It should be noted that a little magnesium arsenate is also added in the White standard-type lamp ($a \approx 0.1$). This gives rise to the low peak in the red in the spectral distribution of this lamp, see fig. 3c.

The colour discrepancy Δ_m of the lamp colour "Warm White" can be reduced in an analogous manner to 0.02 for a value of $a = 0.5$. With the Daylight type lamp the colour discrepancy can be reduced to as low as 0.0075, for $a \approx 0.5$, but in so doing the question of efficiency again becomes significant, so that it has not been found desirable to go further than $a \approx 0.30$, with $\Delta_m \approx 0.025$ for the so-called "Colour Matching" lamp (the colour point being slightly different from that of the standard-type lamp, viz. colour temperature 6500 °K). The values of Δ_m and the corresponding figures of merit are collected in *Table III*.

Table III. Largest remaining colour discrepancies Δ_m and the figures of merit H for the three types of "de Luxe" lamps which were obtained by improving the spectrum in the red with the aid of magnesium arsenate; a = ratio between the two red phosphors.

	a	Improved		Standard	
		Δ_m	H	Δ_m	H
"Cool Daylight"	0.3	0.025	75	0.055	67
"Warm White"	0.5	0.020	84	0.065	62
"White"	0.34	0.023	76	0.05	64

The improved "Warm White" lamp has never been realized in this form; with $a = 0.5$ the efficiency would be undesirably low. (The calculation for this lamp was made starting from a colour temperature of 3100 °K, colour point $x = 0.427$, $y = 0.396$, which was laid down earlier.) The "Colour Matching" lamp has a colour point corresponding to a colour temperature of 6500 °K.

It will be observed that the addition of the red magnesium-arsenate phosphor — in roughly optimum proportions — to all three types of lamps leads to appreciable improvement of the colour rendering qualities. Nevertheless the resulting lamps still do not satisfy the highest demands that can be made in this respect. Attempts were made to approximate more closely to the ideal by taking additional measures to correct the second deficiency mentioned above — the excess in the blue-violet and in the yellow-green.

The absorption of the blue-violet mercury line

An obvious means to reduce the blue-violet hump is to cause a sufficiently strong absorption of the mercury line in the lamp itself. This must be accompanied by an appropriate alteration of the phosphor mixture to eliminate the hump in the yellow-green spectral region, since this hump was only necessary in order to counter the displacing effect of the mercury line on the colour point. The notorious false rendering of yellow and orange objects will then no longer be found.

Experiments involving absorption of the mercury line were being made in Eindhoven as long ago as 1938-39. At that time G. Zecher prepared experimental lamps with uranium-glass walls which absorbed in the desired spectral region. The feasibility of the principle was hereby clearly demonstrated, but its use in practice came up against the impossibility of making tubes with a uniform glass wall of predetermined thickness to regulate the absorption. Experiments on absorbing lacquer layers applied to the outside of the lamp and containing suitable organic dyestuffs failed owing to the same difficulty and owing to well-nigh unavoidable local variations in the lacquer layer. The most attractive solution that remained was to use an inorganic pigment. Many such pigments do not need to be processed in a lacquer; they can be applied to the inner side of the glass wall, since they will withstand the heat treatment during the manufacture of the lamps without decomposing. Here, however, it proved difficult to find pigments with the desired spectral absorption curve.

The investigation took a turn for the better when it was observed that magnesium arsenate, which had been used in supplementing the fluorescence in the red, could be excited not only by the ultraviolet mercury radiation but also by the blue-violet spectral line. This meant that the undesirable radiation was absorbed and that useful radiation was obtained for it. As normally prepared, magnesium arsenate phosphor absorbs the blue-violet line only very weakly but by adopting a special mode of preparation, this absorption can be increased to such an extent that a layer of roughly the same thickness as the normal fluorescent layer

(a few milligrams per cm²) is sufficient to bring about the desired absorption (*fig. 6*). The use of two layers of the phosphor, one absorbing and one non-absorbing, makes it possible to regulate to a

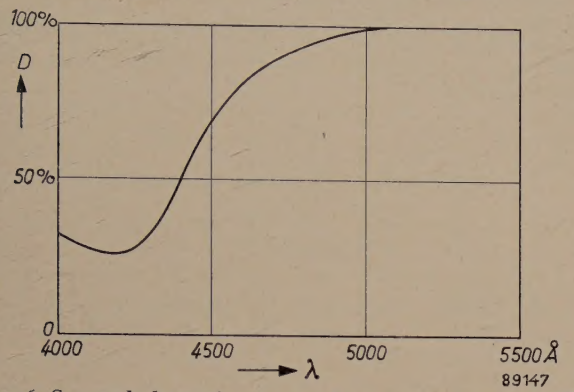

Fig. 6. Spectral absorption curve of magnesium arsenate. The transmission D is plotted as a function of the wavelength λ. The absorption factor referred to in the text is $\delta = |\log D|$. For non-scattering substances this factor is proportional to the thickness of the layer. This likewise applies approximately to magnesium arsenate, although here the absorption is attended with much scattering and with reflection.

certain extent the relative absorption of blue-violet and the fluorescent contribution in the red, independently of each other.

The question now arose as to whether the colour rendering would improve indefinitely with increasing absorption or whether there was an optimum absorption in this respect. Calculations showed that the latter was the case. The calculations were carried out in a manner analogous to that described above in regard to the addition of red; since they are rather time-consuming, we have confined ourselves to one phosphor mixture, the mixture of halophosphate, magnesium arsenate and willemite already referred to. We shall give here a brief outline of these calculations.

A value for the absorption is first chosen. This is characterized by the value $\delta = |\log D|$, where D is the transmission factor for the mercury line $\lambda = 4358$ Å. The transmission curve of the absorbing layer (transmission factor as a function of the wavelength) for the chosen value of δ is derived from fig. 6. The ordinates of the emission curves for the four phosphors used (see above) for each wavelength are then multiplied by the transmission factor, so that four new, effective emission curves are found. Starting from chosen values for the mixing proportion a of the two reddest phosphors, the colour discrepancies Δ_p of the 15 test objects are calculated as before as a function of a (cf. figs. 4 and 5). It is then possible to establish which value for a is the best, and how great is the maximum remaining colour discrepancy Δ_m associated with that value.

This determination of the best possible colour rendering was repeated for various values of δ, and this whole series of calculations was carried out for mixtures of the ("effective") phosphors corresponding to the three lamp colours "Cool Daylight", "White" and "Warm White". The bulky numerical material amassed was processed to give three graphs *fig. 7a, b* and *c*. In these graphs a is plotted along the abscissa and δ along the ordinate, and lines are drawn for constant values of the maximum colour discrepancy Δ_m.

To interpret the graphs we look first at the line $\delta = 0$ (abscissae), which corresponds to the case treated earlier with no absorption. In fig. 7*a* which refers to the Cool Daylight lamp, we see that for $a = 0.35$, the value of Δ_m is 0.02; for $a = 0.49$, $\Delta_m = 0.0075$, while for still higher values of a, Δ_m increases, e.g. $\Delta_m = 0.02$ for $a = 0.6$. If we then take cases in which $\delta > 0$ (with absorption), it can be seen in fig. 7*a* that for $\delta = 0.05$, the discrepancy Δ_m is likewise reduced to 0.0075, a now being 0.47, but that Δ_m does not assume still

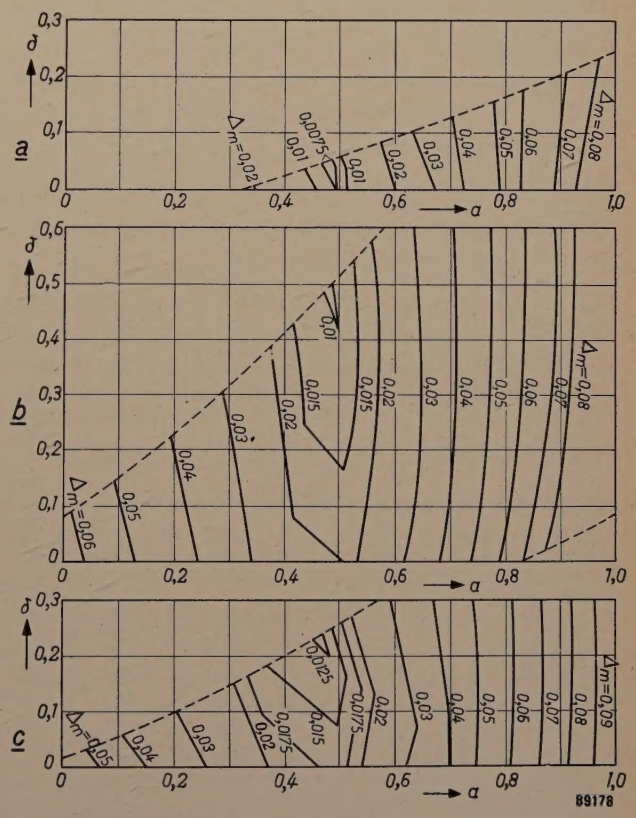

Fig. 7. The greatest remaining colour discrepancy Δ_m in the UCS diagram calculated for the lamp colours *a*) Cool Daylight, *b*) Warm White, *c*) White, with the phosphors halophosphate, magnesium arsenate and willemite; the mixing parameter a is varied and moreover a partially absorbing layer of magnesium arsenate, absorption factor δ for $\lambda = 4358$ Å, has been applied in order to attenuate the blue-violet mercury line.

Lines of constant Δ_m in the a-δ plane are drawn. Outside the broken boundary lines the light contribution of one of the phosphors has negative values, so that the prescribed colour points cannot be realized with those combinations of a and δ.

lower values. This is in agreement with what was to be expected: it has already been pointed out that with the Cool Daylight lamp the second deficiency (blue-violet and green-yellow humps) could not be expected to have any great effect. For this lamp, therefore, correction of this deficiency by absorption does not lead to any noteworthy improvement.

For the lamp colour Warm White the situation is quite different, see fig. 7*b*. Without absorption, $\delta = 0$, Δ_m can at best be reduced to 0.02, for a value of $a \approx 0.5$. With absorption, on the other hand, Δ_m is reduced in the most favourable case to 0.01, i.e. just to the observable limit; the required value of δ for this is 0.4 to 0.5, that of a is again approximately 0.5. Since this is one of the most important results of the whole investigation from a practical point of view, we have collected the numerical values of a number of points in the graph in fig. 7*b* in *Table IV*, together with Harrison's figure of merit for each phosphor mixture with given δ and a. It will be observed that H figures of more than 90 can be attained [13]).

Finally a few words regarding the lamp colour White, for which fig. 7*c* obtains. For $\delta = 0$ (see also fig. 5) the smallest value of Δ_m which can be obtained is 0.017, with $a = 0.5$. Optimum absorption appears to be $\delta = 0.23$, the maximum colour discrepancy with $a = 0.46$ then being reduced to 0.012.

[13]) The fact that both Harrison's figures of merit and the residual maximum colour discrepancies Δ_m are known for a large number of different types of light, makes it possible to test the validity of the figure of merit. With this in view the figure of merit has been plotted as a function of Δ_m in *fig. 8*. Although a fairly large spread can be observed, there is nevertheless a clear correlation between the two quantities (the straight line shown). It can thus be seen that we are justified in employing Harrison's figure of merit, at least in the first instance, for assessing the colour rendering qualities of a fluorescent lamp.

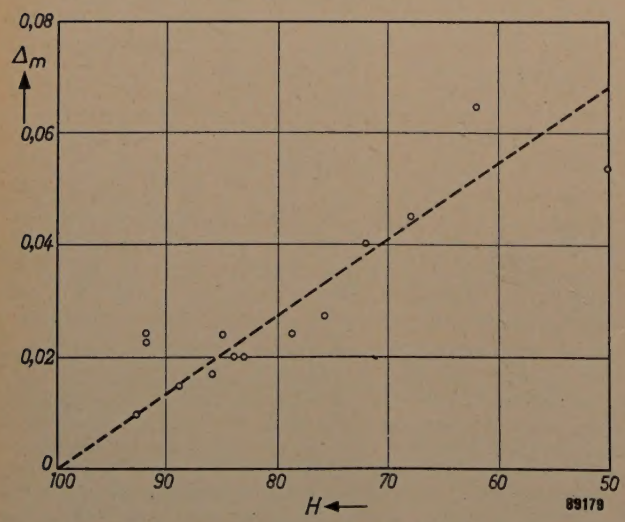

Fig. 8. Maximum colour discrepancy Δ_m plotted against Harrison's figure of merit H, both calculated for a number of phosphor mixtures with the lamp colour Warm White; see Table IV.

Table IV. Calculated maximum colour discrepancies Δ_m and figures of merit H for "Warm White" fluorescent lamps with halophosphate, magnesium arsenate and willemite, with various mixing parameters a for the red light contributions and a varying degree of absorption δ of the blue-violet mercury line. (The blank spaces indicate combinations of a and δ for which one of the constituent phosphors would have to give a negative contribution for the "Warm White" colour point, so that this colour point cannot be realized with these combinations.)

a \ δ	0		0.2		0.4		0.6	
	Δ_m	H	Δ_m	H	Δ_m	H	Δ_m	H
0	0.065	62	—	—	—	—	—	—
0.2	0.045	68	0.040	72	—	—	—	—
0.4	0.024	79	0.020	83	0.017	86	—	—
0.5	0.020	84	0.015	89	0.010	93	—	—
0.6	0.027	76	0.024	85	0.023	92	0.025	92
0.8	0.063	33	0.057	45	0.054	50	0.054	50

Construction of the fluorescent de Luxe lamps; new phosphors

The following sub-sections summarize, with some amplifications, the results thus far achieved and explain their application in a number of de Luxe fluorescent lamps now on the market.

Daylight de Luxe or Colour Matching

The present-day Daylight de Luxe (or Colour Matching) lamp makes use of halophosphate with magnesium arsenate ($a = 0.3$) and willemite, but there is no absorption. Its colour temperature is 6500 °K and its spectral energy distribution is as shown in *fig. 9a*. The maximum colour discrepancy is 0.025 and its luminous efficiency is 50 lm/W.

Although the lamp is satisfactory in practice, better colour rendering, if this could be attained without seriously detracting from the luminous efficiency, would certainly be desirable.

Since absorption is of little avail in this case, improvement must be sought in the application of other phosphors. The most obvious shortcoming that calls for correction is the fairly deep "valley" which still exists between the red maximum of the halophosphates (5800 Å) and that of the magnesium arsenate (6600 Å). A combination of different phosphors with cadmium borate as its principal component was found to answer this purpose well, but was unusable in practice, since the light yield of the borate falls off too rapidly during life.

Warm White de Luxe

In the Warm White de Luxe lamp the combination of halophosphate and magnesium arsenate is used, colour rendering being improved by a layer of magnesium arsenate which is applied between the fluorescent layer proper and the wall of the tube

and which reduces the intensity of the blue-violet mercury line to about $^1/_3$ ($\delta = 0.5$). The spectral distribution of this lamp is shown in fig. 9*b*; the colour temperature is 2900 °K, the maximum colour discrepancy 0.01, the figure of merit 92, the luminous efficiency 47 lm/W. *Table V* shows the spectrum divided up into spectral bands and includes for comparison the spectral distributions of a black body at 2900 °K and of an experimental Warm White de Luxe lamp without absorption. It will be observed that absorption has resulted in a much better approximation to the ideal in the blue-green

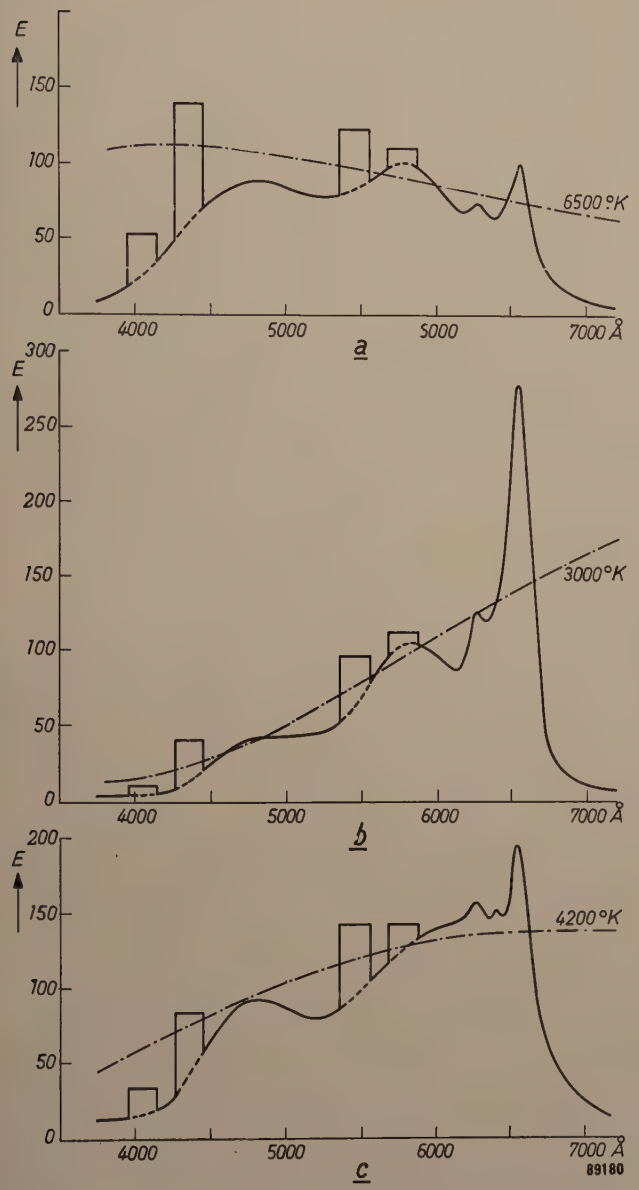

Fig. 9. Spectral energy distribution of fluorescent de Luxe lamps with good colour rendering, which are being produced at the present time.

a) Daylight de Luxe or Colour Matching, with halophosphate, magnesium arsenate and willemite. Colour temperature 6500 °K. $H = 75$; luminous efficiency 50 lm/W.

b) Warm White de Luxe, with the same phosphors and an absorbing layer of magnesium arsenate ($\delta = 0.5$ for $\lambda = 4358$ Å). Colour temperature 2900 °K. $H = 92$; luminous efficiency 47 lm/W.

c) White de Luxe, with calcium strontium silicate, blue halophosphate and magnesium arsenate together with an absorbing layer of magnesium arsenate ($\delta = 0.3$). Colour temperature about 4000 °K. $H = 95$; luminous efficiency 44 lm/W.

As in fig. 3*a-c*, the spectral energy distribution of the corresponding black body is indicated (dot-dash line).

Table V. Distribution of light-flux over eight spectral bands for fluorescent lamps "White de Luxe" and "Warm White de Luxe", the latter both with and without absorption of the blue-violet mercury line. All the lamps employ halophosphate, magnesium arsenate ad willemite. For comparison the distribution for a black body with the corresponding temperature is shown.

Spectral band		"White de Luxe" with absorption	4200 °K	"Warm White de Luxe" without absorption	2900 °K	"Warm White de Luxe" with absorption
No.	Wavelengths in Å					
I	3800-4200	0.005	0.017	0.006	0.006	0.003
II	4200-4400	0.21	0.14	0.31	0.062	0.16
III	4400-4600	0.43	0.50	0.08	0.26	0.22
IV	4600-5100	8.1	8.1	2.0	5.5	4.5
V	5100-5600	37.6	38.6	36.1	33.7	34.1
VI	5600-6100	39.5	39.1	45.5	42.5	44.7
VII	6100-6600	13.7	12.5	15.6	16.4	15.5
VIII	6600-7800	0.57	0.99	0.48	1.54	0.87
Figure of merit H		95	100	81	100	92

spectral bands (III and IV). At the same time it will be seen that it has been possible to enhance the red content (spectral bands VII and VIII) without incurring an increase in the green (V and VI) to keep the colour point constant.

This lamp has been found in practice to come up to all expectations both for use in restaurants, department stores etc., and for use in the home.

White de Luxe

With the mixture of halophosphate and magnesium arsenate it has been found possible to produce a fairly good White de Luxe lamp, especially if absorption is incorporated (up to $\delta = 0.23$). However, it has been found possible to obtain particularly good results by using a phosphor mixture containing a red silicate phosphor, and halophosphates in combination with a layer of absorbing magnesium arsenate which cuts down the intensity of the blue-violet mercury line to about $^1/_2$. The lamp made with this mixture (colour temperature about 4000 °K) is found to give even better colour rendering than the new Warm White de Luxe lamps. Its spectral distribution is shown in fig. 9*c* and the distribution of light flux over the eight spectral bands is given in Table V. The figure of merit is 95 and the luminous efficiency 44 lm/W.

The outline of the development of fluorescent lamps drawn above is not the whole story; it makes no mention of various sidetracks which were followed up for a short while in the laboratory (and occasionally in manufacture) before it was realized that they were leading to a dead end. This account will perhaps have given too strong an impression that in the development of these lamps, the course to be followed was plotted solely by the compass of calculation. If this is so a slight rectification is called for. By making the concept of "colour" with its many physiological complications accessible to calculation, Bouma and other workers in this field have certainly brought us a big step forward; but subjective approval by the user remains the ultimate goal of good colour rendering by any type of lighting. Wide-scale testing under practical conditions, therefore, is the deciding factor in determining whether any new type of lamp shall be manufactured.

Summary. By using a mixture of various phosphors in a tubular fluorescent lamp, the colour point of the lamp in the chromaticity diagram can be varied within wide limits. Three colour points have been chosen for lamps which correspond either to average daylight (colour Cool Daylight, colour temperature 6800 °K), or to incandescent lamp light (colour Warm White, 2900 °K), or to light which lies between the two (colour White, 4200 °K). In addition to the three standard types of fluorescent lamps corresponding to the above, which employ halophosphate phosphor and have optimum luminous efficiencies, other types have been developed, the "de Luxe" lamps (with approximately the same colour temperatures), which have somewhat lower luminous efficiencies, but whose colour rendering has been made as natural as possible. The colour rendering qualities of these lamps have been improved by adding red to the spectrum and attenuating the blue-violet mercury line (this being attended by a reduction of the light contribution in the yellow green). Both effects can be achieved with the aid of a magnesium arsenate phosphor which is prepared in different ways. The general form of the calculations for the determination of the best proportions of mixing and optimum degrees of absorption is outlined. Very good results have been arrived at in this way for the colours Warm White de Luxe and White de Luxe. As regards the Daylight de Luxe or "Colour Matching" lamp, the fact that the luminous efficiency cannot be allowed to suffer unduly for the sake of improvements in the colour rendering makes it preferable to find a solution through a different mixture of phosphors. A new mixture of phosphors combined with absorption by magnesium arsenate has given good results in a new White de Luxe fluorescent lamp.

HIGH-SPEED PHOTOGRAPHS OF THE IMPLOSION OF TELEVISION PICTURE TUBES

The photographs shown here are three of a series taken in connection with tests on the implosion of television picture tubes. The photographs were taken by R. A. Chippendale at the Mullard Research Laboratories, Salfords, Surrey, England.

Implosion was initiated by a steel weight dropped on to the rim of the tube. A conducting graphite strip on the glass triggered the flash-tube (Mullard

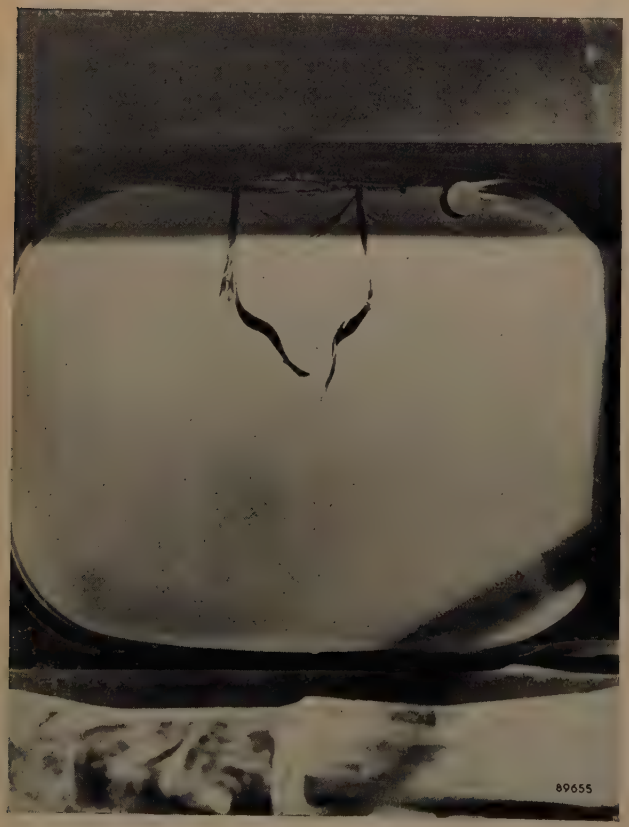

LSD 2) at an early stage of fracture, immediately after impact. Although these photographs are not of the *same* event they broadly represent three steps in the implosion: 1) Initial stage, immediately after impact; 2) 10 msec delay: screen shattered; 3) 100 msec delay: tube disintegrates. In this last case, the usual implosion guard (a glass or acrylic sheet fixed in front of the tube) was removed.

COUNTERS FOR X-RAY ANALYSIS

by P. H. DOWLING *), C. F. HENDEE *), T. R. KOHLER *) and W. PARRISH *).

621.387.4:545.824:548.734

Geiger counters, proportional counters and scintillation counters have played an all-important role as radiation detectors in nuclear physics and allied fields for many years. The Geiger counter was the first of these to enter the field of soft X-rays, and in recent years the other types of counters have been introduced. Faced with a choice between the three types, the worker in the field must know their relative merits and limitations for different applications. Such an assessment is given in this article, on the basis of the physical properties of the counters and of practical measurements under a variety of conditions **).

Introduction

About 15 years ago Geiger counters adapted to the detection of relatively soft X-rays were introduced into the general X-ray diffraction field as a substitute for photographic film. The most striking feature of the counter tube in this field is its superiority to film in the evaluation of relative radiation intensities. This has led to the successful development of the method of "diffractometry" and related procedures. Three articles on this subject recently published in this Review may be quoted [1] [2] [3]).

The development of the Geiger counter for X-ray detection has been followed in recent years by the adaptation of the *proportional counter* and the *scintillation counter* to the same purpose [4]). Detectors of this type and their associated circuits, suitable for X-ray diffractometry and X-ray spectrochemical analysis, have been developed and engineered in the Philips Laboratories at Irvington in such a form that they can be readily substituted for the Geiger counter tube on the "Norelco" X-ray goniometer. Each of the three detectors thus available has its specific advantages and, of course, limitations. In *fig. 1* the three detectors and the complete interchangeable units are shown. A description of the new detectors will be given and their underlying mechanisms and essential characteristics will be discussed in this article.

The Geiger counter

For the sake of comparison, the design of a Geiger counter tube for X-ray detection, which has been described on several occasions in this Review, should be briefly recapitulated.

A cross-section of the standard "Norelco" Geiger counter tube, type 62019, is shown in *fig. 2*. The tube consists of a chrome-iron cathode cylinder 2 cm in diameter, along whose axis a 0.75 mm tungsten anode wire is mounted. The tube is filled with argon gas to a pressure of 55 cm Hg, and a small amount (less than 0.4%) of chlorine is added as a quenching agent. Approximately 1400 V is applied between cathode and anode. X-rays enter the tube axially through an end window of mica 0.013 mm thick. An X-ray quantum will give rise to a discharge pulse in the tube if it is absorbed in the gas within the active volume, which is a cylinder around the anode wire about 10 cm long (practically the whole length of the tube) and 1.2 cm in diameter. When copper Kα radiation ($\lambda = 1.54$ Å, quanta of energy 8 keV) is used, in a beam not wider than the active volume, about 60% of the X-ray quanta impinging on the tube window are detected. This percentage is called the *quantum counting efficiency* of the counter tube.

The quantum counting efficiency depends on the absorption of the radiation by the active gas column. The effect of absorption by the tube window and by the adjoining inactive part of the gas column (which, however, in the 62019 type of tube is

*) Philips Laboratories, Irvington-on-Hudson, N.Y., U.S.A.

) The subject-matter of this article was presented in part at the 3rd Congress of the International Union of Crystallography, Paris, July 1954. Cf. also Acta cryst. **7, 626, 1954.

[1]) W. Parrish, E. A. Hamacher and K. Lowitzsch, The "Norelco" X-ray diffractometer, Philips tech. Rev. **16**, 123-133, 1954/55.

[2]) W. Parrish, X-ray intensity measurements with counter tubes, Philips tech. Rev. **17**, 206-221, 1955/56 (No. 7-8).

[3]) W. Parrish, X-ray spectrochemical analysis, Philips tech. Rev. **17**, 269-286, 1955/56 (No. 10).

[4]) Proportional counter:
S. C. Curran, J. Angus and A. L. Cockroft, Phil. Mag. **40**, 36-52, 1949.
G. C. Hanna, D. H. W. Kirkwood and B. Pontecorvo, Phys. Rev. **75**, 985-986, 1949.
W. Bernstein, H. G. Brewer Jr. and W. Rubinson, Nucleonics **6**, Feb. 1950, pp. 39-45.
Scintillation counter:
F. H. Marshall, J. W. Coltman and A. I. Bennett, Rev. sci. Instr. **19**, 744-770, 1948.

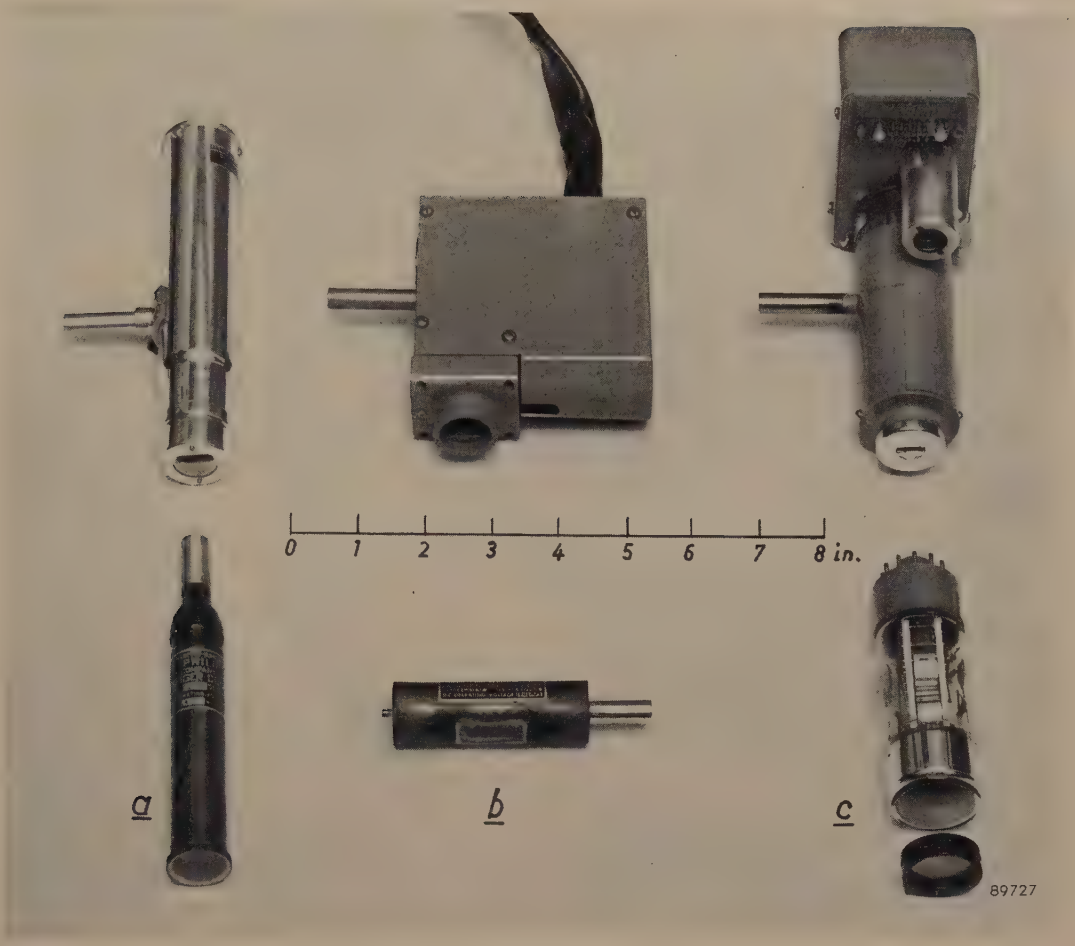

Fig. 1. Interchangeable X-ray detectors for the "Norelco" equipment. *a*) Geiger counter, type 62019. *b*) Xenon-filled proportional counter, type 62031. *c*) Scintillation counter, type 52245.

The proportional and scintillation counter have cathode follower circuits, which are mounted directly with the counter on the goniometer arm. The complete detector units are shown in the upper part of the photograph.

only about 3 mm long) limits the efficiency. Since both the desirable and the undesirable absorption are a function of the wavelength of the radiation, the quantum counting efficiency depends strongly on the wavelength. This is a most important factor for practical applications, as will be discussed below.

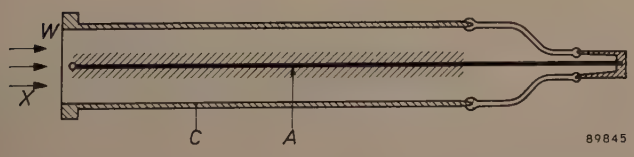

Fig. 2. Cross-section of "Norelco" Geiger counter tube, type 62019. The tube is filled with argon (55 cm Hg) and a small amount of chlorine. A voltage of about 1400 V is applied between cathode *C* and anode *A*, the permissible voltage range ("plateau") is more than 300 V wide. X-rays (*X*) enter axially through an end window *W*, the active volume of the tube is indicated by shading. The useful life of the tube is practically unlimited; even after having counted 10^9 quanta, a tube of this type showed no deterioration of characteristics.

The spectral response of the argon-filled Geiger counter tube, type 62019, as calculated from absorption data [5]) and which has been confirmed by measurements [6]), is shown in *fig. 3.*

The detailed mechanism of quantum detection in a Geiger counter tube can be described briefly as follows [7]). Absorption of a quantum by a gas atom

[5]) J. Taylor and W. Parrish, Rev. sci. Instr. **26**, 367-373, 1955 (No. 4).

[6]) W. Parrish and T. R. Kohler, Rev. sci. Instr. **27**, 795-808, 1956 (No. 10).

[7]) See for instance: D. H. Wilkinson, Ionization chambers and counters, Cambridge Univ. Press, 1950. Also: N. Warmoltz, Philips tech. Rev. **13**, 282-292, 1951/52. — It should be noted that Geiger counter detectors for nuclear experiments in which β-rays or very hard X-rays (γ-ray quanta of millions of eV energy) are to be measured, have a somewhat different mechanism: the quanta in these cases are absorbed — generally to a rather low percentage — in the cathode wall or in the anode, not in the gas. The development of the discharge is similar to that in the detector for soft X-rays described here.

results in the ejection of a photo-electron. The gas ion so produced gets rid of its excess energy in most cases by emitting one or more additional high-energy electrons (internal conversion by the Auger process).

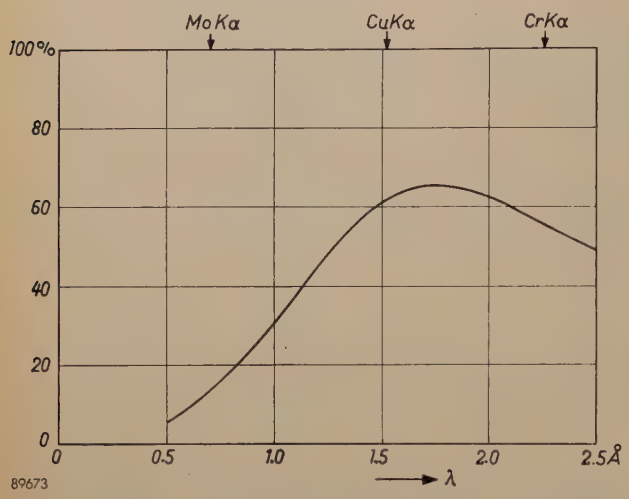

Fig. 3. Quantum counting efficiency as a function of wavelength (spectral response) for the argon-filled Geiger counter, calculated from absorption data [5]).

These conversion electrons as well as the photo-electron in turn spend their kinetic energy by forming ion pairs in the gas. Thus, a total number of about 310 ion pairs are formed in argon by the absorption of one copper Kα quantum. Each of the secondary electrons will give rise to a Townsend avalanche owing to acceleration in the electric field of the counter tube. Metastable atoms and photons emitted from the avalanches cause the emission of still more electrons throughout the tube, so that a self-sustained discharge filling the whole volume of the tube is started. The discharge is quenched after a short time either by the action of an external quenching circuit causing the tube voltage to drop as the discharge current is built up, or by the action of the quenching agent added to the gas (self-quenching).

The latter action can be explained as follows. Most of the ionization occurs near the central wire, where the electric field strength is largest. The electrons thus formed are quickly attracted to (collected at) the central wire, leaving behind a positive ion space-charge sheath around the wire, which effectively lowers the electric field strength in the gas and momentarily prevents further ionization. The positive ion sheath drifts out from the wire, restoring after a short time ("dead time") the original field conditions. This would allow the discharge to be reinitiated by other electrons subsequently emitted from the wall; such an emission, however, is prevented by the quenching agent.

The gas amplification process described results in discharge pulses of large amplitude, say 1-10 V, a feature which makes the Geiger counter an extremely useful radiation detecting device for many problems. The "dead time", on the other hand, limits the usefulness of this device. During this time another quantum entering the tube cannot give rise to a separate pulse and so is not detected. As a result a proportion of the arriving quanta is not counted, and this proportion increases with their arrival rate, i.e. the response becomes non-linear at large radiation intensities. The dead time of the Geiger counter type 62019 is 170 μsec; the "effective" dead time for CuKα-radiation produced by an X-ray tube operated on a 35 kV (peak) full-wave rectified voltage [8]) is 270 μsec, so that appreciable deviations from linearity ($> 8\%$) occur at counting rates as low as 500 counts per second. Individual intensity values (peak values of diffraction lines) can be corrected for the non-linearity effect. No practical correction is possible, however, when the number of quanta is measured during a period of *varying* radiation intensity, as, for example, in the measurement of "integrated line intensities" [9]).

The proportional counter

The large pulse size and the long inactive period of the Geiger counter both originate from the spreading of the discharge throughout the volume of the tube. In the proportional counter, whose design is basically similar to that of the Geiger counter, the voltage on the tube is chosen *below* the threshold value for the self-sustained discharge (i.e. the lowest limit of the Geiger plateau), and the discharge is then essentially confined to a plane normal to the axis of the tube, located where the original X-ray quantum was absorbed. The discharge current in this case is only the sum of the Townsend avalanches of the secondary electrons. The "gas amplification factor" therefore is about 10^4, as against 10^6 or 10^7 in the Geiger counter tube, and the pulses produced are rather small. Because of the limited extent of the discharge, however, nearly the whole volume of the tube remains active and can detect a second X-ray quantum absorbed shortly after the first. In fact, two quanta need be separated only by about 0.2 μsec, i.e. the electron collection time, in order to be separately detected. When the average current of the counter tube is used as a measure of the quantum arrival rate, it is even unnecessary to have separated

[8]) Loc. cit. [2]), p. 218.
[9]) Loc. cit. [2]), p. 216.

pulses; linearity is then maintained up to extremely high counting rates, say 10^7 counts/sec or more. (At still higher rates, the increasing space charge lowers the effective field.)

Since the pulses produced in the proportional counter are approximately 10^3 times smaller than those of a Geiger counter, an amplifier having a gain of approximately 10^3 must be added in order to bring the pulses to the level required for operating the counting circuits (about 0.25 V). Evidently, this is the price paid for better linearity.

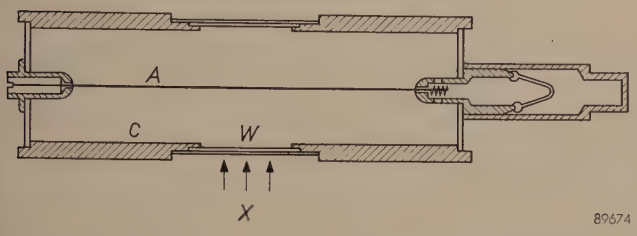

Fig. 4. Cross section of "Norelco" proportional counter, type 62031. *A* anode wire, *C* cylindrical cathode. This counter is filled with xenon (32 cmHg); a small quantity of methane is added as a discharge-limiting agent. About 1700 V is applied, the required voltage being dependent on the radiation measured. X-rays *X* enter through a *side* window *W*. Unabsorbed quanta leave the tube through a window diametrically opposite the entrance window. (Not all proportional counters are fitted with this exit window.)

A well-known property of the proportional counter, which is responsible for its name, is the proportionality between the size of the pulse and the energy of the absorbed quantum. In fact, whereas the pulses of a Geiger counter vary only slightly in size, the original quanta acting merely as triggers, the pulses delivered by a proportional counter each represent a charge equal to a fixed multiple (the gas amplification factor) of the ionization produced by the absorbed quantum, and hence are proportional in size to the quantum energy. This proportionality is a very useful characteristic since it enables the elimination of undesired radiation components by the method of pulse height discrimination. We shall deal with this point at some length in this article.

The "Norelco" proportional counter pictured in fig. 1, and whose cross-section is shown in *fig. 4*, is fitted with a 0.013 mm mica window of size 0.6×1.6 cm in the *side wall* of the cathode cylinder, with the X-ray beam entering perpendicularly to the wire. This design is adopted to ensure the proportionality just mentioned: in order to make the gas amplification factor for all quanta as nearly equal as possible, the spatial distribution of the electric field should be identical for all quanta, irrespective of the place where they are absorbed. (At the ends of the cylindrical tube considerable distortions of the equipotential surfaces are unavoidable.) Moreover, the "Norelco" tubes are made approximately four times longer than the diameter, in order to enhance the uniformity of the field distribution in the vicinity of the window, and any disturbing effect of the mica window itself is avoided by covering its interior wall with either a very thin film of evaporated gold or a thin sheet of beryllium. In some tubes an exit window of size 0.8×1.7 cm is placed diametrically opposite the entrance window to allow the unabsorbed portion of the X-ray beam to leave the tube without striking the chrome-iron cylindrical cathode wall and possibly causing X-ray fluorescence.

The unabsorbed portion of the beam of course should be made as small as possible. This was the very reason why in the early days of diffractometry the end window design was introduced for the argon-filled Geiger counter X-ray detector, ensuring a long active gas column. The shorter length of the absorption path in the side-window design is compensated by selecting a heavier gas, in most cases *xenon*. The proportional counter, type 62032, filled with pure xenon to a pressure of 32 cmHg, has practically the same quantum counting efficiency for CuKα as the Geiger counter 62019. In fact, the efficiency of both tubes is nearly identical in the whole spectral region between about 0.5 and 2.5 Å; cf. *fig. 5*. Higher gas pressures are not desirable because the operating voltages increase rapidly with pressure and would exceed the range of the "Norelco" power supply.

If the internal gas amplification at which the counter is operated is increased too far, the tube may go into continuous discharge. Moreover, even before this point is reached, oscillations in the form

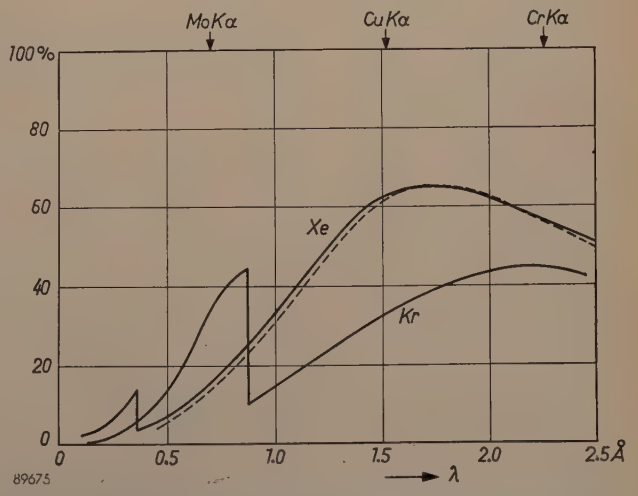

Fig. 5. Spectral response of the proportional counter filled with xenon (curve *Xe*) and with krypton (curve *Kr*), calculated from absorption data [5]). The dotted line is the spectral response of the Geiger counter from fig. 3.

of "after-pulses" occur after each normal X-ray pulse. The relative amplitudes of the after-pulses increase with voltage and may be sufficient to operate the scaling circuit, thereby falsifying the measured counting rate. It is therefore essential to keep the internal gas gain below some maximum value. It has been our experience that the operating voltage therefore should be chosen such as to produce pulses not exceeding 1 millivolt. (This should apply to the most energetic X-ray quanta — desired or not — which are absorbed in the counter, since the amplitude of the after-pulses increases with the quantum energy.) Hence it is necessary in practice to use a rather high external (amplifier) gain.

The after-pulsing phenomena and the difficulties involved in using high gain amplifiers (especially when pulse height discrimination is used) can be avoided by the addition of methane or some other organic gas to the noble gas of the proportional counter. The "quenching" or "limiting" agents prevent secondary processes and limit the discharge to a single avalanche. Thus, with the "quenched" proportional counter ("Norelco" type 62031) a higher gas amplification can be used, which allows much greater flexibility in the equipment and technique.

Since the limiting agent will gradually decompose, the quenched proportional counters have a limited useful life, whereas pure gas counters have an extremely long life. The useful life attained by tubes with not more than 10% methane, however, is adequate for all practical purposes (at least 1 or 2 years, in average practice).

Proportional counters filled with *krypton* have been used for the detection of MoK radiation. The spectral response curve for the krypton-filled counter, which is also shown in fig. 5, reveals a better quantum counting efficiency in the 0.8 Å wavelength region, due to the KrK absorption edge. The otherwise much lower absorption of krypton is in part compensated by increasing the gas pressure to 50 cmHg.

Using a krypton-filled proportional counter for the detection of MoKα X-rays brings to prominence a phenomenon which is of considerable importance for measurements requiring pulse height discrimination, viz. the "escape peak". This will be discussed in the section on pulse height discrimination, where the concept of "energy resolution" will also be introduced. Since this concept as well as the phenomenon of the escape peak are of like importance in the scintillation counter, the latter should first be described.

The scintillation counter

The scintillation counter is composed of two basic elements: a flat fluorescent single crystal, and a photomultiplier tube (*fig. 6*). A NaI-crystal activated by Tl (1%) is commonly used for soft X-rays. An X-ray quantum absorbed by an atom of the crystal produces a photo-electron and usually

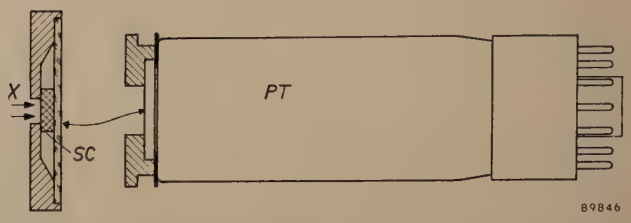

Fig. 6. Schematic representation of the scintillation counter, type 52245. The scintillating NaI.Tl-crystal (*SC*) is mounted in a light-tight holder, fitted with a glass cover transmitting the scintillation light to the end of the photomultiplier tube (*PT*) and an X-ray window (beryllium foil) at the other side.

one or more Auger electrons, which on their tracks energize a large number of fluorescent centres located at the sites of Tl ions in the crystal lattice. Each fluorescent center thus energized may emit a visible photon. The light so obtained is directed onto the cathode of the photomultiplier tube by reflecting surfaces near or on the crystal. For roughly 10 of these photons one electron is liberated from the cathode. The photomultiplier owing to its secondary electron emission gain of 10^5 or 10^6 delivers a current pulse which after amplification is suitable for operation of the counting circuits.

The scintillation counter as adapted to soft X-rays has characteristics similar to the proportional counter in two respects: it has an extremely short dead time (about 0.2 μsec), ensuring linear counting up to very high intensities; and its pulse amplitudes are proportional to the quantum energy, thus offering the possibility of pulse height discrimination. The outstanding feature of the scintillation counter as compared to both the Geiger and the proportional counter is its high quantum counting efficiency (nearly 100%) and its almost uniform spectral response in the wavelength region 0.2 - 2.5 Å. This is shown in *fig. 7* for a crystal 1 mm thick. The quantum counting efficiency of nearly 100% is due to the practically complete absorption of the soft X-rays in the NaI-crystal slab [10]). Much thinner crystals of NaI could be used for X-ray analysis owing to its very high X-ray absorption coefficient. The area

[10]) The efficiency of scintillation counters in their "native" field, viz. nuclear physics, is rarely higher than say 1%, owing to the very incomplete absorption of the hard nuclear radiations in crystals of reasonable size.

of the crystal need be only slightly larger than the cross-section of the X-ray beam.

Other characteristics which make the NaI-crystal particularly suited for the purpose, are the following. Its spectral emission curve matches the sensitivity curve of photomultiplier tubes rather well; it has a high optical transparency; its fluorescence decay constant is very small, about 10^{-7} sec, which accounts for the short dead time mentioned above; it is easily grown in single crystals of sufficient size and uniform transparency. The one important disadvantage of NaI.Tl is that it is extremely hygroscopic. The crystal therefore is hermetically sealed in an aluminum holder, which itself is completely opaque to external visible light. For good transparency to the incident X-rays, the front of the holder exposed to the beam is provided with a 0.13 mm thick beryllium window. The other side of the crystal mount has a flat glass plate and is "wrung" onto the photomultiplier tube face, with a fluid film of high refractive index (Dow Corning fluid 200) in order to minimize reflection losses. For the same reason the inner surfaces of holder and beryllium X-ray window are highly polished. Since beryllium is difficult to polish, the side of this window next to the crystal is sometimes covered with a very thin ($\sim$ 1 μ) bright aluminum foil. (It should be noted that light losses do not affect the quantum counting efficiency, but do impair the energy resolution, see later.)

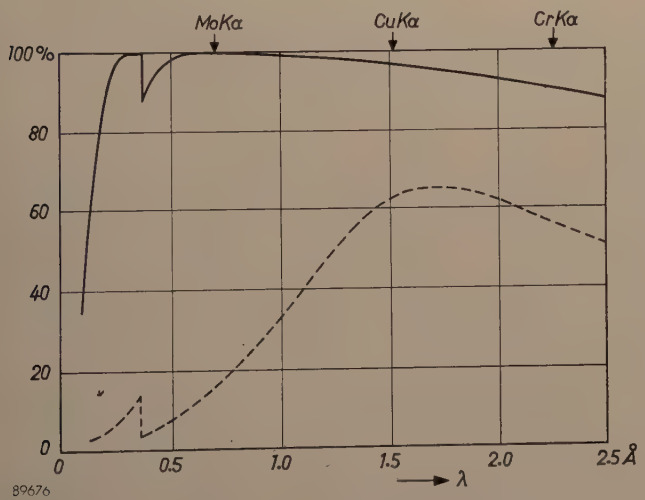

Fig. 7. Spectral response of the NaI.Tl scintillation counter type 52245, calculated from absorption data [5]). The dotted line is the response curve for the xenon-filled proportional counter from fig. 5.

The decrease of the spectral response curve of the scintillation counter in fig. 7 towards short wavelengths is due to the harder X-rays passing through the thin crystal without being absorbed. The decrease towards longer wavelength, however, is caused by the increasing absorption of the beryllium window. Windows of better transparency at wavelengths greater than 3 Å are conceivable, but for the very soft X-rays the scintillation counter is difficult to use because the pulses become very small and it becomes difficult to distinguish them from the noise generated by the photomultiplier tube.

From this it will be clear that the photomultiplier tube should be designed for a very low noise ("dark current" caused e.g. by ohmic leakage, thermionic and field emission, gaseous ionization). Cooling the photomultiplier in order to reduce thermionic emission is not necessarily of benefit in reducing the noise, since in many photomultiplier tubes the noise pulses of largest amplitude, and hence the most troublesome ones, arise from gaseous ionization.

Other characteristics of the photomultiplier, such as the electron yield per incident photon and the total electron gain, have been mentioned above. Suitable types of photomultiplier tubes require anode voltages of 850 to 1400 V. The scintillation counter shown in fig. 1 is operated with an amplifier of gain 250 to 1000, depending on the voltage applied to the photomultiplier tube. The useful life of the scintillation counter is practically unlimited.

Pulse height discrimination

Pulse height discrimination as applied in X-ray diffractometry and X-ray spectrochemical analysis has the object of measuring radiation of a single wavelength, i.e. one specific diffraction line or one specific spectral emission line, while radiation of other wavelengths is eliminated [11]). The pulses delivered by a proportional or scintillation counter are fed via a linear amplifier (output pulse proportional to input pulse) with adjustable gain to a single-channel pulse height analyzer. This may be set to pass all pulses greater than a given amplitude (base) or only those pulses lying within a specified, rather narrow amplitude range (channel width or "window"). The pulses passed by the analyzer are fed to a recording counting-rate meter [2]).

A striking example illustrating the usefulness of pulse height discrimination is found in the diffractometry of *radioactive* samples [12]). Owing to the large size of the specimen used in diffractometry, the detector in the case of a radioactive sample is

[11]) The general methods of pulse-amplitude analysis and the apparatus used cannot be described in this article. See e.g.: A. B. van Rennes, Pulse-amplitude analysis in nuclear research, Nucleonics **10**, July 1952, pp. 20-27, and August 1952, pp. 22-28. See also [6]).

[12]) D. J. Knowles, 10th Pittsburgh Conf. X-ray Electr. Diffr. 1952, p. 32. T. R. Kohler and W. Parrish, X-ray diffractometry of radioactive samples, Rev. sci. Instr. **26**, 374-379, 1955 (No. 4).

exposed to an intense background radiation. Shielding of the detector by lead (and scanning by moving the X-ray tube, with its heavy shield, instead of the detector) is a possible but cumbersome solution. If, however, a scintillation or proportional counter is used, the vast majority of pulses produced by the β- or γ-rays have amplitudes different from those produced by the diffracted X-rays (they may be larger as well as smaller); they can therefore be largely eliminated by a pulse height discriminator with the window set for the energy (wavelength) of the diffraction line whose intensity is to be measured.

Energy resolution of different detectors

When a given radiation is being measured while the upper and the lower amplitude limits of the analyzer window are continuously shifted in synchronism with the recording chart (keeping a constant window width), a graph of the *pulse amplitude distribution* of the pulses of the detector is obtained. *Fig. 8* shows the pulse amplitude

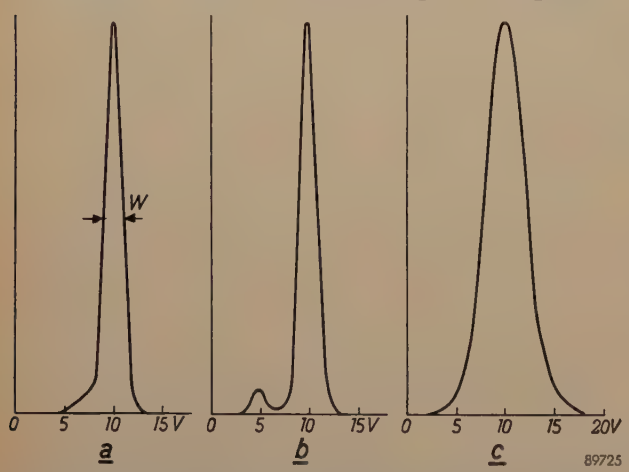

Fig. 8. Amplitude distribution curves of the pulses generated by CuKα radiation in *a*) krypton-filled proportional counter, *b*) xenon-filled proportional counter, *c*) scintillation counter.

distribution curves, obtained with a window 0.5 V wide, for three types of detectors exposed to *monochromatic* radiation (CuKα, which gives 10 V pulses). Each curve exhibits a peak of finite width, which means that even quanta of a single energy (i.e. 8 keV) produce pulses of different amplitudes, varying around an average value; this value corresponds to the true quantum energy. The variation, which limits the power of the detector to separate quanta of closely spaced wavelengths, is due to the statistics of the ionization or excitation and amplification processes involved. The separating power, or "energy resolution" (which of course cannot be enhanced by a narrower analyzer window) is measured by W/A, W being the width at one half peak height of the pulse amplitude distribution curve and A the average pulse amplitude (roughly the abscissa of the centre of the peak).

In fig. 8 it is seen that the energy resolution W/A for CuKα radiation is much better for the proportional counter, filled with xenon or krypton, than for the scintillation counter. The better resolution of the proportional counter can be understood as follows. One CuKα quantum will produce an average number m of 350 ion pairs in the xenon-filled proportional counter. Owing to fluctuations of m and of the gas amplification factor for each electron, the resulting pulse amplitude fluctuates with a relative standard deviation σ/A, which can be shown [13]) to amount to about $\sqrt{1/m}$. Using the relation $W = 2.36\ \sigma$, the ratio W/A is calculated to be 13% for $m = 350$. The actual value measured in mass-produced counter tubes is about 20% (irregularities of the anode wire and slight asymmetry in its centering, which cause fluctuations of the gas amplification, probably account for the difference). In the scintillation counter, one CuKα quantum will produce about 500 visible photons in the NaI.Tl crystal [14]), but only about $n = 25$ of these photons give rise to an "electron avalanche" in the photomultiplier tube. (The other photons are ineffectual because either they do not arrive at the photocathode, or they fail to liberate an electron, or the liberated electron fails to reach the first dynode, or because of fluctuations in the secondary emission process at the dynodes [15]).) The relative standard deviation again is $\sigma/A \approx 1/\sqrt{n} = 1/\sqrt{25}$, so that $W/A = 2.36\ \sigma/A = 47\%$. Thus the ratio W/A for the scintillation counter is in this example about 2.5 times larger and its energy resolution about 2.5 times smaller than that of the proportional counter. Significant improvements in the energy resolution of both these types of detectors do not appear likely at present.

From the relations $W \propto 1/\sqrt{m}$ and $W \propto 1/\sqrt{n}$ implied in the above it is seen that for both types of counter tubes $W/A \propto 1/\sqrt{A}$: the energy resolution improves with the square root of the quantum energy

[13]) U. Fano, Phys. Rev. **72**, 26-29, 1947; O. R. Frisch (unpublished); S. C. Curran, A. L. Cockroft and J. Angus, Phil. Mag. **40**, 929-937, 1949.

[14]) About 20% of the quantum energy is converted into visible light; the quantum wavelength is 1.54 Å, the average wavelength of the visible emission is 4100 Å, so that the number of visible photons per X-ray quantum is $0.2 \times 4100/1.54 \approx 500$. — It should perhaps be noted that the limited energy-conversion efficiency (20%) does not detract from the nearly 100% quantum counting efficiency of the scintillation counter for CuKα, mentioned earlier: practically every absorbed quantum will be *counted* anyhow, independent of the loss of large part of its energy in the crystal.

[15]) G. A. Morton, RCA Rev. **10**, 525-555, 1949.

of the detected radiation (i.e. — within obvious limits — inversely with the square root of its wavelength).

When the composition of the radiation to be measured and the behaviour of the detector are not known, the desirable setting of the pulse height analyzer window may be quickly determined by using only the base of the analyzer (i.e., with the upper limit of the window inoperative, see above) and making a recording with synchronized base shift and chart movement. This will yield what is called the "integral curve" (number of pulses per second having an amplitude exceeding the value on the axis of the abscissa). The integral curves obtained for CuKα radiation with the same three detectors as in fig. 8 are reproduced in *fig. 9*.

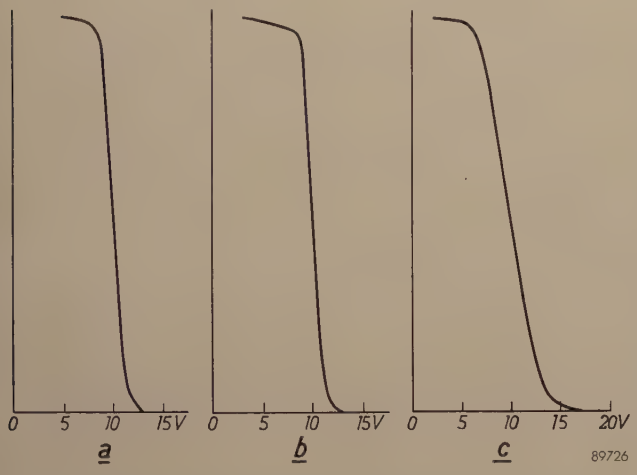

Fig. 9. Integral curves of the same pulses as in fig. 8. The ordinate of each curve indicates the number of pulses per second having an amplitude exceeding the voltage value plotted as abscissa.

The escape peak

The primary process in the absorption of an X-ray quantum by all the counter tubes considered is the ejection of an electron from an inner shell of a gas or crystal atom. This photo-electron will originate say from the K shell, if the wavelength of the absorbed quantum is shorter than that of the K absorption edge of the atom. The following transition of an L shell electron to the K shell vacancy is associated with either the ejection of one or more other electrons (Auger process) or the emission of a new X-ray quantum (fluorescence). It has been stated above that the Auger electrons similarly to the photo-electron will ultimately be absorbed in the gas, or crystal, and will contribute to the formation of ion pairs, or to the excitation of fluorescent centres. The alternative fluorescent X-ray quantum, however, has a sizable probability of *escaping* from the gas or crystal, especially since its wavelength is always somewhat longer than that of the absorption edge and absorption for these quanta is therefore relatively weak (cf. figs. 5 and 7). For the Geiger counter it does not matter greatly whether a substantial proportion of the original energy E_i of the quantum manages to escape as fluorescent energy, E_f. For the proportional and scintillation counter, however, the escaping of fluorescent X-radiation has the undesirable consequence that some of the original quanta result in pulses with a "wrong" amplitude, viz. proportional to $E_i - E_f$ instead of E_i. Thus two peaks appear in the pulse distribution curve for monochromatic radiation, the main peak (at $V_i \propto E_i$) and the "escape peak" (at $V_e \propto E_i - E_f$).

A small escape peak is visible in fig. 8*b* for CuKα radiation incident on the xenon-filled proportional counter. A very large escape peak — larger than the main peak — is found when MoKα radiation ($E_i = 17.4$ keV) is measured with a proportional counter filled with krypton (the escaping fluorescent KrKα radiation has $E_f = 12.6$ keV). This is illustrated by *fig. 10*.

The existence of the escape peak will influence practical measurements with pulse height discrimination in two ways. Since the analyzer window usually has to be made so narrow that it will reject pulses of the escape peak, the quantum counting efficiency will be correspondingly reduced. The loss would amount to about 55% in the case of *fig. 10*. Secondly, for quanta $E_i + E_f$, if present, the escape peak would inevitably be passed by the analyzer window set for the main peak of quanta E_i; the discrimination against unwanted radiation (e.g. a continuous background) is therefore incomplete.

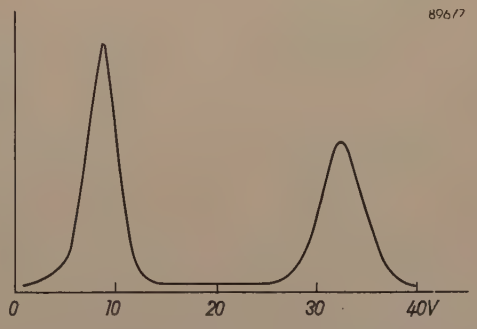

Fig. 10. Amplitude distribution of the pulses produced in the krypton-filled proportional counter by MoKα radiation (quantum energy $E_i = 17.4$ keV). The pulses forming the "main peak" have amplitudes (average 32 V) corresponding to the ionization produced by both photo-electron and Auger electron(s). The amplitudes of the other group of pulses (average 9 V), forming the "escape peak", correspond to the residual ionization when fluorescent X-rays are lost. The amplitude *difference* (23 V) between pulses of main peak and escape peak is determined by the energy E_f of the escaped fluorescent X-ray quantum (KrKα, with $E_f = 12.6$ keV) and therefore remains constant when the wavelength of the detected radiation is varied.

In some cases the escape peak can be put to good use, since the energy resolution of the counter is better in this part of the pulse amplitude distribution curve than in the main peak. This can be seen as follows. Consider the problem of separating, in spectrochemical analysis, two closely spaced emission lines, of quantum energies E_{i_1} and E_{i_2}, and assume that the detector delivers an escape peak for each line, the energy of the escaping fluorescent quantum being E_f. The mean pulse amplitude A_e of the escape peak in each case is smaller than that of the main peak A_m by the same amount ΔA, proportional to E_f. Thus the escape peaks of both radiations have the same separation as the main peaks, $A_{e_1} - A_{e_2} = A_{m_1} - A_{m_2}$. The half height width W of any peak in the pulse amplitude distribution, however, is proportional to the square root of the mean amplitude, $\sqrt{A}$ (see above). Each escape peak, therefore, is narrower than the main peak by a factor $\sqrt{A_e/A_m}$. Evidently the narrower escape peaks with equal separation can be more easily resolved than the main peaks.

quantum counting efficiency of the proportional counter is low at these short wavelengths.

Incidentally, it is seen in this recording that one radiation may produce several escape peaks. In fact, besides Kα fluorescent quanta, Kβ quanta and in other cases L quanta may arise, with their corresponding fine structure. Usually these niceties can be disregarded.

Comparison of the three types of detectors in practical applications

When using the "Norelco" X-ray instrumentation, it is necessary to choose for each problem the most suitable detector among the three available types. The considerations determining this choice will now be discussed. In doing so, it seems logical to start with X-ray spectrochemical analysis: shortcomings

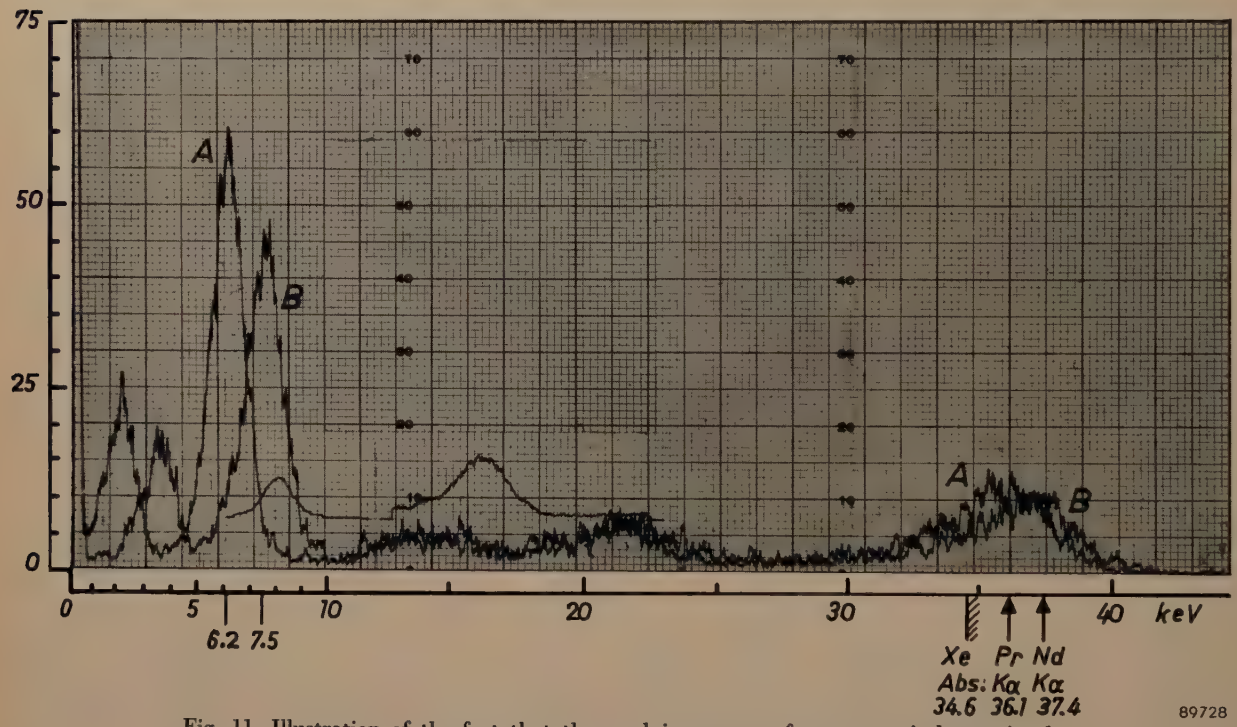

Fig. 11. Illustration of the fact that the resolving power of a counter is better in the escape peak region than in the main peak region. The pulse amplitude distribution curves A and B were obtained from a xenon-filled proportional counter with monochromatic radiations of energies 36.1 keV (praseodymium Kα) and 37.4 keV (neodymium Kα) respectively.

Use can be made of this fact by setting the window of the pulse height analyzer for one of the two escape peaks rather than for one of the two main peaks.

A striking example is seen in *fig. 11*, which shows the pulse amplitude distribution curves of a xenon-filled proportional counter for the Kα radiations of praseodymium (atomic number 59, $E_i = 36.1$ keV) and neodymium (atomic number 60, $E_i = 37.4$ keV). Both radiations have wavelengths shorter than the K-absorption edge of xenon and produce a very strong escape peak (85% of the total number of output pulses are grouped in this peak!). Since $E_f = 28.9$ keV for Xe Kα, it is calculated that the escape peak width is about 0.5 times the main peak width. It should be noted, however, that the

of the Geiger counter for this particular application gave the fillip to the introduction of proportional and scintillation counters into the X-ray field, so that here the case is rather clear-cut.

Spectrochemical analysis [3])

In spectrochemical analysis, radiations of *different* wavelengths, whose intensities may vary greatly, must be compared quantitatively or semi-quantitatively. The non-linearity of the Geiger counter due to its long dead time is a serious dis-

advantage in this case, since it will generally necessitate a correction of the measured peak intensities. Such a correction is neither easy nor accurate, particularly because the operational dead time of the counter when the X-ray tube is not supplied with a constant potential but e.g. with a full-wave rectified voltage, will depend on the wavelength [16]). For intensities exceeding a few thousand counts/sec (intensities exceeding 10^5 counts/sec may occur), corrections are no longer possible and it will be necessary to reduce the intensities to the Geiger counter range by controlled absorption. This becomes very difficult for a series of different wavelengths.

Both the proportional and the scintillation counter have much better linearity than the Geiger counter. Their dead time (~ 0.2 μsec) would cause non-linearity only at 10^7 counts/sec or even higher. The practical limits of linearity in this case are set by the associated electronic circuits. The standard "Norelco" scaling circuit gives rise to a count loss of 10% at 14000 counts/sec. New circuits now available are linear to 1% at 10000 counts/sec. Similarly the pulse height analyzer hitherto used in our investigations precluded the measurement of counting rates higher than about 5000 counts/sec, owing to a shift of the base level depending on the counting rate. Better analyzers are now available which retain the simplicity of the present instrument but permit intensity measurements up to about 15000 counts/sec or even higher, depending upon the counting rate of the pulses being rejected by the analyzer.

The strongly wavelength-dependent quantum counting efficiency, which the proportional counter shares with the Geiger counter (fig. 7), requires corrections to the measured intensities when characteristic lines of elements several atomic numbers apart are compared and no reference standards are used, as is frequently done in qualitative and semi-quantitative analysis. Although there are several other factors which influence the relative line intensities, it is an important advantage of the scintillation counter for spectrochemical analysis that owing to its nearly uniform spectral response, corrections for variations in the efficiency are not necessary. Even more important is its very high value of the quantum counting efficiency, particularly for wavelengths < 1 Å. This advantage is directly reflected in the time necessary for each measurement, since a fixed number of counts must be accumulated for a given accuracy (cf. [2])); the counting rate obtained with the scintillation counter exceeds that of the xenon-filled proportional counter by a factor of almost 2 for CrKα and of about 12 for AgKα.

For long wavelengths the scintillation counter loses its advantage owing to the rather large photomultiplier noise mentioned previously. Measurements with all types of counters are hampered here by the difficulty of making sufficiently transparent X-ray windows. Using non-vacuum-tight windows in special flow counters has extended the useful range of the proportional counter with its inherent low noise to about 12 Å (in a helium path goniometer, cf. [3])): Kα lines of silicon (7.13 Å), aluminum (8.34 Å), magnesium (9.89 Å) and sodium (11.91 Å) could thus be measured with a good peak-to-background ratio [17]), whereas the longest wavelength for which we were able to make useful measurements with the scintillation counter, using a specially selected crystal and photomultiplier tube, was Kα of sulphur (5.37 Å). TiKα (2.8 Å) is about the longest wavelength that can be measured in routine fashion with the standard "Norelco" scintillation counters.

The possibility of pulse height discrimination with the scintillation counter and proportional counter is a great asset in spectrochemical analysis when peak intensities become smaller. Thus the analysis of minor and trace amounts of elements is achieved with better accuracy and lower limits of detectability. The usefulness of pulse height discrimination for separating overlapping spectral lines of different elements has been discussed in a previous article [3]), as well as the possibility of a non-dispersive spectrochemical analysis based on those principles. Clearly the greater energy resolution of the proportional counter may be advantageous in these cases, although one must balance this advantage against the higher quantum counting efficiency of the scintillation counter for short wavelengths.

Powder diffractometry [1])

The situation in diffractometry is quite different from that in spectrochemical analysis, for two reasons: the intensities to be measured are usually much lower, and in principle use is made of monochromatic radiation, e.g. CuKα (1,54 Å) or MoKα (0.71 Å) or CrKα (2.29 Å). The Bragg reflections of this radiation obtained from the specimen (sharp

[16]) For a given peak voltage on the X-ray tube, the fraction of the a.c. cycle during which the elements in the specimen can fluoresce and into which, therefore, the quanta to be counted are bunched, decreases as the atomic number increases. Thus the effective dead time becomes longer for regions of shorter wavelengths.

[17]) C. F. Hendee, S. Fine and W. Brown, Rev. sci. Instr. **27**, 531-535, 1956 (No. 7). Prof. C. H. Shaw of Ohio State University, according to a personal communication, has reached about the same limit by using proportional counters with a beryllium foil window.

lines) are superimposed on a background consisting chiefly of two contributions: radiation of a continuous spectrum, which is unavoidably emitted by the X-ray tube and *scattered* by the specimen, and characteristic *fluorescent* X-radiation excited in the specimen [18]). The scattered continuous background has its maximum intensity at wavelengths usually much shorter than the useful radiation. A fluorescent background — which will appear only if the specimen contains elements whose excitation voltage is sufficiently low — has wavelengths shorter or longer than the useful radiation. The total intensity and the spectral distribution of the background thus may vary widely, depending on the specimen, the X-ray tube voltage and other experimental conditions.

Counter tubes for powder diffractometry should have a high quantum counting efficiency, because of the low intensity of most diffraction lines, and should yield a high peak-to-background ratio, for the measurement of weak lines. Linearity it usually of less importance, and so is the uniformity of the spectral response. The non-uniform spectral response of the Geiger counter (and proportional counter) in fact may be regarded as an advantage for some applications of powder diffractometry, since it produces a crude sort of monochromating effect, which eliminates a large part of the short-wavelength continuous scattered background. A qualitative conclusion is that for many applications of diffractometry, especially when simplicity of equipment matters, the Geiger counter offers a very satisfactory solution. Nevertheless, the scintillation counter, using more elaborate equipment, is capable of even better peak-to-background ratios: the lack of the above-mentioned monochromating effect is overcome by pulse height discrimination. The high quantum counting efficiency of the scintillation counter is another advantage. This efficiency, on the other hand, is diminished when pulse height discrimination is applied: the pulse height analyzer window, set for the peak in the pulse amplitude distribution curve for the monochromatic radiation used (fig. 8), will transmit only a certain percentage of the relevant pulses owing to the finite peak width. The quantum counting efficiency multiplied by the "transmission factor", will be called the "detection efficiency". Making the window wider will increase the transmission factor and therefore the detection efficiency, but reduce the monochromating effect.

From the above it will be clear that for choosing the best detector for any particular application of powder diffractometry, a *quantitative* comparison of the detection efficiency and the peak-to-background ratio obtained with each of the three types of detectors is necessary. Giving equal importance to these two quantities, their product may be calculated and used as a "*figure of merit*" of the detector. A large number of measurements have been made in order to establish these figures of merit for a variety of cases [6]).

As a first instance, a typical inorganic specimen was selected and measurements were made using the three radiations previously mentioned above.

[18]) It is assumed that non-specimen scatter, due to misalignment of the goniometer, is practically eliminated. The contribution of air scatter can usually be neglected, In addition to the continuous radiation, a portion of the useful monochromatic radiation is scattered (not "reflected") by the specimen. This contribution to the background of course cannot be distinguished from the diffraction line proper by pulse height discrimination. — A possible non-X-ray background, as in the diffractometry of radioactive samples [12]), need not be considered here.

Table I. Comparison of detectors for powder diffractometry. Measurements performed on the (111) reflection of a pure silicon powder specimen (no fluorescent background). For each of the three X-ray tubes (target Mo, Cu and Cr respectively) the voltage was empirically selected so as to give the highest ratio of useful characteristic to undesired "white" radiation. The pulse height analyzer window was set for a transmission factor of about 0.90. The Geiger counter measurements were corrected for dead time losses (τ = 270 μsec). The figures of merit are relative values, with the first in each group arbitrarily taken as 100.

Detector	MoKα, 55 kV$_p$, 7 mA; filter Zr 0.002″; peak P at 2Θ = 13.0°; background B at 10.0°; beam apert. 2α = 0.5°			CuKα, 40 kV$_p$, 9.6 mA; filter Ni 0.0007″; peak P at 2Θ = 28.4°; background B at 20.0°; beam apert. 2α = 1.0°			CrKα, 30 kV$_p$, 12.8 mA; filter V_2O_5; peak P at 2Θ = 42.9°; background B at 35.0°; beam apert. 2α = 2.0°		
	Det. eff. %	P/B	Figure of merit	Det. eff. %	P/B	Figure of merit	Det. eff. %	P/B	Figure of merit
Scintillation counter with pulse height discrimination	90	44	100	89	134	100	90	93	100
Scint. counter without pulse ht. discr.	100	10	25	100	12	10	100	5	6
Prop.c. (Xe) with pulse ht. discr.	12	44	13	56	146	69	58	92	64
Prop.c. (Xe) without pulse ht. discr.	13	16	5	63	57	30	60	16	11
Prop.c. (Kr) with pulse ht. discr.	12	51	15	33	64	18	—	—	—
Prop.c. (Kr) without pulse ht. discr.	29	29	21	36	26	8	—	—	—
Geiger counter	14	27	10	51	46	20	59	18	13

The specimen gives no measurable fluorescence with any of these radiations. The results are listed in *Table I*. For MoKα the superiority of the scintillation counter over the other detectors is very marked; this evidently is due to its much higher quantum counting efficiency at this wavelength. The figure of merit of the krypton-filled proportional counter is seen to be lowered when pulse height discrimination is applied. This fact is caused by the strong escape peak, whose suppression reduces the detection efficiency more than is gained in the peak-to-background ratio. For CuKα and CrKα the scintillation counter with pulse height discrimination also rates as the best detector but not by so wide a margin as in the case of MoKα. When pulse height discrimination is not applied, the advantage of the Geiger counter (and of the Xe proportional counter) in not being sensitive to the short-wavelength scattered radiation is clearly seen; the Kr proportional counter has a very low figure of merit in this case owing to the rise of its quantum counting efficiency at the KrK absorption edge (fig. 5), and for similar reasons the figure of merit of the scintillation counter *without* pulse height discrimination is low for CuKα and CrKα. The effectiveness of pulse height discrimination in the latter case is very clearly illustrated by *fig. 12*.

It is interesting to note that the peak-to-background ratios obtained with the scintillation and Xe proportional counter are several times higher for CuKα and CrKα than for MoKα. The reason for this is that the characteristic MoKα line is nearly at the peak of the continuous spectrum, whereas the CuKα and CrKα lines are well removed from the peak [19]).

A second series of measurements, which will not be reported here in detail, was concerned with the scattered backgrounds in the diffractometer patterns of different (non-fluorescent) specimens, measured at several diffraction angles. The total background without pulse height discrimination varied by a factor of 20 among the specimens tested. The reduction of total background by the use of pulse height discrimination varied from a factor of about 2 (specimen hexamethylene tetramine) to 53 (specimen silver), for the scintillation counter [6]). Dis-

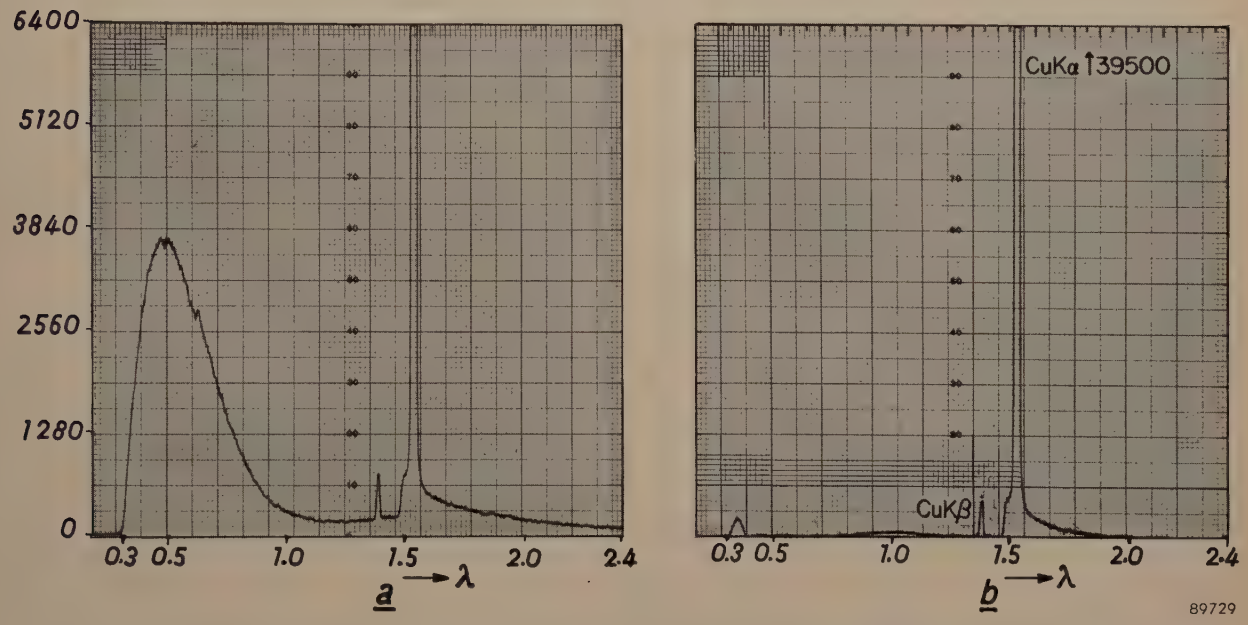

Fig. 12. Spectrum from Cu-target X-ray tube (40 kV_p, full-wave rectification) obtained with scintillation counter and silicon ((111) plane) analyzer crystal, *a*) without, *b*) with pulse height discrimination, the window being set for CuKα with a transmission factor of 0.90. A Ni-filter 0.0007″ thick, which virtually eliminates the CuKβ line and also reduces the continuum, was employed in both cases. The nearly complete suppression of the continuous spectrum in (*b*) is responsible for the enormous improvement in the peak-to-background ratio in diffractometer measurements of polycrystalline specimens with CuKα, as shown in Table I (increase from 12 to 134). Incidentally, the small residual hump at about 0.35 Å is due to the escape peak phenomenon: radiation of wavelength $\sim$ 0.35 Å owing to this phenomenon will produce a certain proportion of pulses falling within the analyzer window set for 1.54 Å.

[19]) W. Parrish and T. R. Kohler, A comparison of X-ray wavelengths for powder diffractometry, J. appl. Phys. **27**, 1215-1218, 1956 (No. 10).

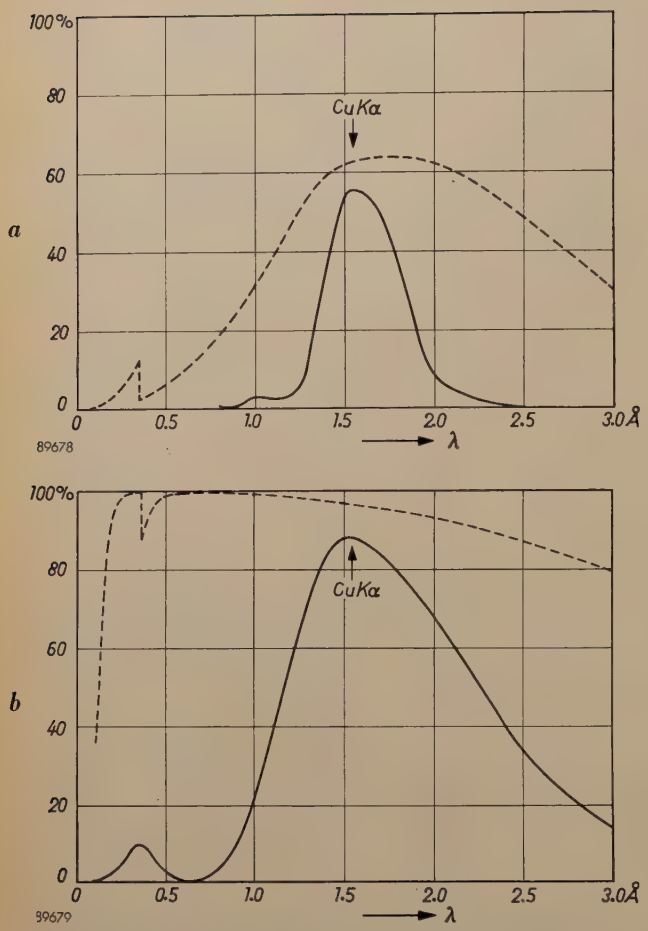

Fig. 13. Detection efficiency for monochromatic radiations as a function of λ, with symmetrical pulse height analyzer window (transmission factor 0.90) set for CuKα. *a*) Proportional counter filled with xenon. *b*) Scintillation counter. The data are calculated from the quantum counting efficiencies (dotted curves, as in fig. 7) and the pulse amplitude distribution curves.

crimination with the Xe proportional counter gives a smaller reduction factor, as may be expected from its lower quantum counting efficiency in the short wavelength region.

Finally a number of measurements were made concerning the background due to specimen *fluorescence*. The diffraction pattern of iron powder obtained with Cu Kα radiation was selected as a rather difficult case. The background from the lower level, resulting in an *asymmetrical* window will decrease the detection efficiency for FeKα by a larger factor than that for CuKα. A ratio of 25 is obtained with the asymmetrical window indicated iron specimen contains strong FeKα and FeKβ fluorescence, in addition to a certain amount of scattered short wavelength continuum. The FeKα wavelength (atomic number 26, $\lambda = 1.93$ Å, energy 6.4 keV) is rather near that of CuKα (atomic number 29, $\lambda = 1.54$ Å, energy 8.0 keV). The efficiency of pulse height discrimination in suppressing the undesired FeK radiation when the window is set for CuKα will in this case largely depend on the energy resolution of the counter. Quantitative evaluation of the effect of discrimination is simpler for such a case than for the suppression of a continuous background, since the quantum counting efficiencies for only two wavelengths need be considered. The ratio of the detection efficiencies for these two wavelengths (i.e. CuKα/FeKα) takes the place of the previously introduced peak-to-background ratio, and the figure of merit is redefined for this case as the product of this ratio times the detection efficiency for CuKα.

The detection efficiency of a counter as a function of wavelength for a given setting of the analyzer window is easily calculated from its spectral response curve (fig. 7) and the pulse amplitude distribution curve for monochromatic radiation (for example fig. 8). The result is shown in *fig. 13a* for the xenon-filled proportional counter, in fig. 13*b* for the scintillation counter. In both cases a symmetrical window setting with a transmission factor of 0.90 was used.

The result looks rather disappointing: a CuKα/FeKα ratio of not more than 1.2 is obtained with the scintillation counter and of 1.6 with the proportional counter. It is not essential, however, to use the above-mentioned *symmetrical* setting of the pulse height analyzer window. Consider the integral curves of the proportional counter for CuKα and for FeKα radiation, *fig. 14*. The symmetrical window setting is indicated by vertical lines; a higher setting of the

Table II. Reduction of fluorescent background with pulse height discrimination (iron specimen, irradiated by radiation of copper target X-ray tube operated at 40 kV(peak); other experimental conditions see fig. 14).

	Symmetrical analyzer window		Asymmetrical analyzer window	
	Ratio of detection efficiencies CuKα/FeK	Figure of merit	Ratio of detection efficiencies CuKα/FeK	Figure of merit
Xe proportional counter	1.6	13.5	25	100
Scintillation counter	1.2	16.3	4.1	27.5

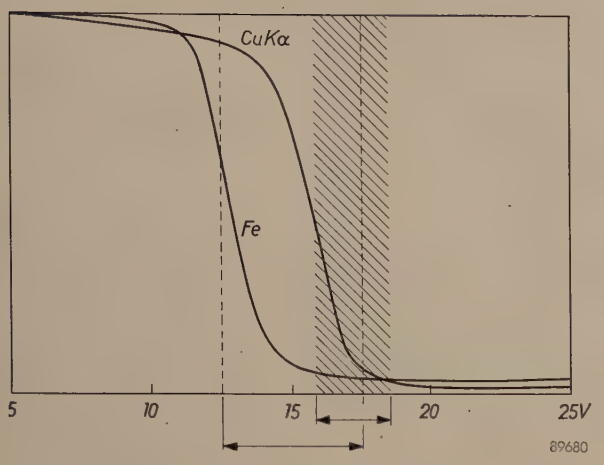

Fig. 14

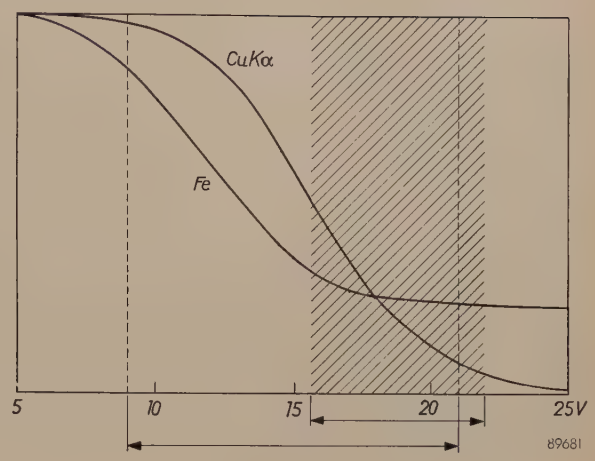

Fig. 15

Fig. 14. Integral curves of the pulses obtained from the xenon-filled proportional counter with CuKα radiation (diffracted (111) peak of a silicon powder specimen) and with background of a pure iron specimen at $2\Theta = 23°$; FeK fluorescence is predominant in this case. The vertical lines indicate the conventional symmetrical setting of the pulse height analyzer window (transmission factor 0.90). Experimental conditions: copper target X-ray tube, 0.0008″ nickel filter for suppression of CuKβ, beam aperture $2\alpha = 1°$, receiving slit width 0.024″. The tube was operated at 20 kV(peak) for silicon and at 40 kV(peak) for iron. The curves were normalized to have the same counting rate at 5 V pulse amplitude (this is permissible since only the relative attenuations caused by the analyzer are considered)

Fig. 15. Same as fig. 14, but for the scintillation counter. The smaller slope of the curves as compared with fig. 14 is due to the poorer energy resolution of the scintillation counter; the higher intensity level at pulse amplitudes above about 18 V (scattered short wavelength continuum) is due to the higher quantum counting efficiency of this counter at short wavelengths.

lower level, resulting in an *asymmetrical* window will decrease the detection efficiency for FeKα by a larger factor than that for CuKα. A ratio of 25 is obtained with the asymmetrical window indicated by shading in fig. 14. A similar but less spectacular improvement is obtained when an asymmetrical window is used for the scintillation counter, as shown in *fig. 15*. The results are summarized in *Table II*.

The smaller improvement with the scintillation counter is a consequence of its poorer energy resolution. On the other hand, even the better resolution of the proportional counter may prove inadequate when smaller wavelength differences occur, as with Co K fluorescence (atomic number 27) excited by CuKα radiation. In that case the use of a crystal monochromator placed after the specimen would be necessary in order to remove all the fluorescent background; the pulse height analyzer may then be omitted and because of its simplicity a Geiger counter will preferably be used for the detection of the monochromatic radiation, especially since the intensities in this case will be rather low. This example is perhaps a fitting conclusion for this article, since it reintroduces the eldest member of the family of X-ray counters and clearly illustrates that each member has specific applications in which it is superior to the others.

Summary. A Geiger counter, a xenon- or krypton-filled proportional counter and a scintillation counter are available as interchangeable detectors for the "Norelco" X-ray goniometer. The design and counting mechanism of each of these detectors is briefly described in this article. The main characteristics of the three detection methods are: the Geiger counter has large pulse amplitude and concurrent simplicity of equipment; the proportional and scintillation counters have linear response up to very high counting rates, and proportionality between pulse amplitude and quantum energy, offering the possibility of pulse height discrimination; moreover the scintillation counter has the highest quantum counting efficiency and a very uniform spectral response, whereas the proportional counters have a better energy resolution. After a discussion of some aspects of pulse height discrimination, especially energy resolution and the escape peak phenomenon, an attempt is made to evaluate the relative merits of the different types of detectors for several applications. For spectrochemical analysis, the scintillation counter will in most cases be preferred for wavelengths up to about 3 Å. For longer wavelengths a very thin window proportional counter (either sealed off or flow type) is desirable. For powder diffractometry, the equal importance of high sensitivity and good peak-to-background ratio leads to the proposal of a figure of merit, which is calculated for different counters and for a typical non-fluorescing specimen analyzed with three radiations (CuKα, MoKα and CrKα). The scintillation counter used in conjunction with pulse height discrimination has by far the highest figure of merit for MoKα radiation; its superiority above the xenon-filled proportional counter is less pronounced for CuKα and CrKα radiation. Finally, a fluorescent specimen (iron powder analyzed with CuKα) is considered. Pulse height discrimination in this case is especially effective when an asymmetrical setting of the analyzer window is used, and the xenon-filled proportional counter is markedly superior to the scintillation counter owing to its better energy resolution.

A MUSICAL INSTRUMENT FOR DEAF-MUTE CHILDREN

789.983:616.28-008.15

Deaf-mute children usually have only very little left of their hearing faculty. Nevertheless, they can perceive sounds of an intensity above a certain threshold value, either through their ears or as vibrations felt by any part of the body, particularly the thorax. If the children grow up as "deaf-mutes", i.e. have not learned to speak and are consequently retarded in their mental development, the reason is largely that they do not realize without instruction that the vibrations they perceive are capable of containing information.

By exercising the sense of vibration in the body it is frequently possible to awaken in deaf-mute children an awareness of the world of sound. It is worth while exploiting these possibilities to the full, for anything that can be done to enable a deaf-mute child to acquire impressions of sound, however imperfect, will contribute to its spiritual development and help it to overcome the almost insuperable difficulties of becoming a "normal" child.

One of the numerous methods at present being employed for training deaf-mute children to exercise their sense of vibration is to play music to them and, more important still, to let them make music themselves. A wind instrument is the most suitable for this purpose since it can also help the children to learn breath-control. Persons able to hear and speak normally are generally unaware of how fundamental this factor is in speech. One of the most important tasks in giving speech instruction to deaf-mute children is to teach them how to control their breathing [1]).

About 15 years ago, some pupils of the Institute for the Deaf at St.-Michielsgestel in Holland were taught to play the clarinet, the vibrations of which can be felt both between the lips and in the chest. It was found that the children began spontaneously to hum the melody they had learned to play on the clarinet [2]). However, the intensity with which they could hear themselves playing this instrument was too weak to lead to sound perception, and moreover very young children, and older ones too, find the clarinet too difficult to play. For this reason the Institute requested our laboratory to develop a wind instrument that would be easy to play and that would enable the children to feel (and, where possible, to hear) the music with their ears by means of headphones and also to feel it over their bodies by means of loudspeakers.

The instrument developed in response to this request is shown in the adjoining photograph [3]). It is a wind instrument but the notes are selected on a keyboard and reproduced electronically. Rather as in a mouth organ, the pitch of the notes is determined by a row of steel reeds mounted on aluminium housings. The pupil blows down a rubber pipe with a glass mouthpiece, and sets the reeds vibrating by depressing keys which open corresponding valves. In the enclosed space containing the reeds a piezo-electric microphone picks up the vibrations, which are then reproduced at the required level via an amplifier and a loudspeaker. The acoustic screening of the microphone was found to be sufficient to prevent acoustic feedback.

Thus, as with the clarinet and other woodwinds, the notes are formed by depressing keys, but now only one finger is needed and a simple keyboard is provided. The intensity of the notes, their start and duration, and thus also the rhythm, are controlled by the breath. In this connection the shape of the mouthpiece is thought to be of particular importance. For this reason (apart from hygienic considerations) the mouthpieces are interchangeable; a broad flange determines the correct position in the mouth.

The problem of condensation and saliva encountered in the playing of wind instruments was solved in this case by Hoeymans [3]) with a simple bellows arrangement, which works as follows. An enclosed space is divided into two chambers by a light, moveable flap, sealed at the edges by thin leather bellows. When air is blown into the one chamber, a nearly equal amount of air is forced out of the other by the displaced flap and this air sets the reed vibrating via the valve opened by the depression of a key. When the player stops blowing, a valve in the second (dry) chamber opens, allowing air from outside to be sucked in by the flap as it re-

---

[1]) Experiments by S. Woldring of the Philips Research Laboratory, Eindhoven, shortly to be published in the "Ned. Tijdschrift voor Doofstommenonderwijs" (Netherlands Journal on the Teaching of Deaf-Mutes) have made this abundantly clear. To read seven short sentences, two normal children had to take 4 and 6 breaths respectively, whereas three deaf children drew respectively 26, 20 and 40 breaths. The breath curves given in the above paper show the unchecked, irregular nature of the deaf children's breathing.

[2]) A. van Uden, Annual Reports of the Institute for the Deaf, St.-Michielsgestel, e.g. 1951, p. 60. For a more general introduction see also: A. van Uden, Rhythmic training in sound perception of severely deaf children, Conf. Nat. Coll. Teachers of the Deaf of Great Britain, Blackpool, 13 April 1955.

[3]) The instrument has been further developed and a number of them built by an Eindhoven music teacher, Mr. A. Hoeymans.

turns to its equilibrium position under the action of a weak spring. This valve closes automatically as soon as air is blown in again, whereupon the displaced air again passes to the reeds. Although it is not possible with this arrangement to produce a long sustained note, owing to the limited stroke of the bellows, Hoeymans has nevertheless evolved a design such that this does not prove troublesome in normal use.

The instrument, which has been in use for several years at the St.-Michielsgestel Institute, serves for individual tuition as well as for class instruction (see photograph overleaf). In the latter case the children can also hear (or feel) and join in the music played by the others.

Some idea of the practical results obtained with this instrument is given by the following data, taken from reports published by A. van Uden [4]).

Two groups of deaf-mute children — with approximately the same loss of hearing, viz. more than 100 dB — had to learn by heart six different melodies; the one group had the instrument described here to play on, while the other group learnt simply by feeling and hearing the melodies. After respectively $3^1/_2$ and 4 hours of practice, the first group was able to recognize the tunes to more than 90%, the other only to 67%; it made hardly any difference in either case whether the children listened to the music with or without a hearing aid. After an interval of five weeks the two groups were again tested to see if they could still recognize the melodies: the results this time were 86% and 33% respectively. "The motor reactions of the first group were more complete than those of the second: head, trunk, arms and hands were spontaneously moved in time with the music."

Among the deafest children from the third up to the seventh class, who had been playing the instrument for more than six months, 24 were tested on their ability to distinguish between the pitch of different notes. The children were told what pitch interval would be used, and they were to discern when the high and when the low note was played. The outcome was 84% correct answers for the major third, 77% for the minor third, 74% for the major second and 72% for the minor second. The percentage of correct answers for the different ages was: 67% in the third class, 73% in the fourth, 89% in the fifth, 74% in the sixth and 79% in the seventh.

4) See the Reports mentioned in footnote [2]). We are indebted to Mr. Van Uden and Sister Irena for information on the pitch and chord perception tests.

Analogous tests on the acquired ability to distinguish between chords, made on 10 of the deafest children, produced even more remarkable results. In 92% of all cases (12 tests per child) the difference was recognized between a fifth and a second; in 89% between a fifth and a third, in 85% between a fourth and a third, in 81% between a third and a second. Even the difficult differences were recognized between a major second and a minor second (68% of all cases) and between a fifth and a fourth (67% of all cases).

One cannot properly appreciate the problems of teaching the deaf and dumb until one has first sat through a number of lessons in an institute such as that mentioned in this article. After such an experience it is difficult to write objectively on the technical side of the subject without digressing on the human aspect. Those of us with normal hearing have good reason to be thankful for the easy way in which we have been able to learn to speak and to understand music and thereby develop our mental faculties normally.

R. VERMEULEN.

SMALL BALLASTS FOR FLUORESCENT LAMPS

621.327.534.15.032.434

In general, the designer of fixtures for fluorescent lamps requires that the ballast be as small and light as possible, in order that the fixtures themselves may be economical of materials and attractive in form. However, if the circuit, the type of lamp, the mains voltage and the frequency are fixed, the dimensions of a ballast cannot be reduced — unless special precautions are taken — without this having undesirable consequences: the losses in the ballast and the temperature of the insulation both increase with decrease in dimensions; greater losses mean a lower efficiency and the higher temperature means that for a given insulating material the ballast will have a shorter life.

These deleterious consequences may be quantitatively estimated as follows [1]). Consider a well-designed ballast and imagine all its linear dimensions to be reduced to $1/p$ times their original values ($p > 1$): the volume and weight then fall to $1/p^3$ of their original values. If the power of the lamp is kept constant, then the losses in the copper and iron of the reduced ballast become p times as great owing to the higher current density and the greater magnetic induction, respectively. This greater loss is dissipated as heat through a p^2 times smaller surface, so that the rise in the temperature of the insulation will be p^3 times greater. If it is required to reduce the volume by, say, 25% ($p = \sqrt[3]{4/3} = 1.10$), then an increase in total loss of 10% and an increase in the rise of temperature of 33% must be expected. The fairly low increase in the loss can sometimes be compensated by more careful design or by using a better magnetic material; the increase in the rise of temperature, however, can only be avoided by ensuring appreciably greater heat removal.

The heat which develops in the coils and cores is transmitted to the walls of the box in which the ballast is mounted, and thence via the fixture to the surroundings. The construction of the fixture and the thermal contact between the box wall and the fixture are highly important in this connection, but will not be discussed in this article since the ballast designer has no direct say in the matter. He can, however, try to make the difference in temperature between the hottest point in the insulation and outside surface as small as possible. For this to be the case, the whole of the space between core-coil assembly and box wall must be filled with a material which is a good conductor of heat. This material, moreover, must have a number of other properties. In general it is required of the filling material that it should

a) conduct heat efficiently,
b) be a good electrical insulator,
c) damp the acoustic vibrations,
d) be moisture-repellent,
e) penetrate well into narrow spaces between the components,
f) not soften at high temperatures,
g) have a low thermal expansion, and
h) be cheap.

We shall now see how far a few of the common filling materials come up to the above requirements.

A material frequently used is asphalt in the form of a casting compound. The coefficient of thermal conductivity of asphalt is about 10^{-3} W cm^{-1} °C^{-1}. By admixing quartz sand, ground quartz (which is finer in grain), aluminium oxide or a similar substance, the thermal conductivity can be increased by a factor of 3 to 6. Since the dissipation of choke coils and transformers of ballasts per unit surface area is about 0.1 W/cm^2, a temperature gradient of 10 to 5 °C will occur if the average thickness of the asphalt around the components is 3 mm.

An objectionable property of asphalt, however, is its softening at high temperatures. If the box is completely full, asphalt will be forced out through the seams in the box as a result of thermal expansion. Moreover, the components of the ballast may sink in the soft asphalt, possibly causing short-circuits if they are not attached to the box; and, preferably, in order to avoid hum, they should not be fixed to the box. A way around this is to leave some space in the box and to interpose pieces of insulating paper between the components and the box walls (*fig. 1*), but then the heat transfer suffers appreciably.

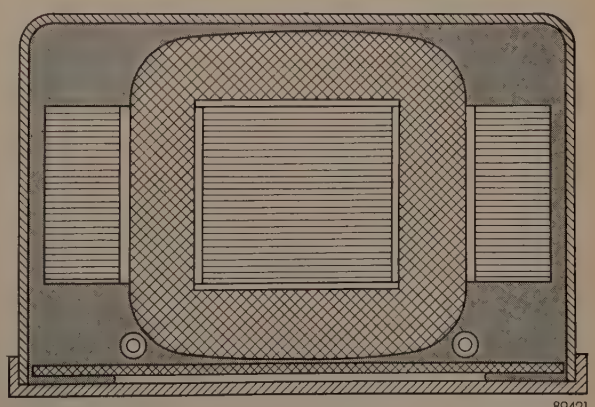

89421

Fig. 1. Cross-section of a ballast filled with asphalt.

[1]) Cf. C. Zwikker, Fluorescent lighting, Philips Technical Library, Eindhoven 1952, p. 128.

The search for a filler which would not soften led some five years ago to the use of aluminium foil. The coefficient of thermal conduction of aluminium is some 300 times greater than that of the best asphalt filler mass. The temperature gradient would therefore be negligibly small if a solid aluminium filling were used. Technically, however, this is not feasible; a large part of the advantage must be sacrified, since the aluminium has to be in some easily worked form and since the coil has to be enclosed in good electrical insulation. This led to the choice of aluminium foil which has been dimpled in a regular pattern by a previous treatment and is packed into the spaces between the components in the box in packets or in layers (*fig. 2*). In this way, using only a small

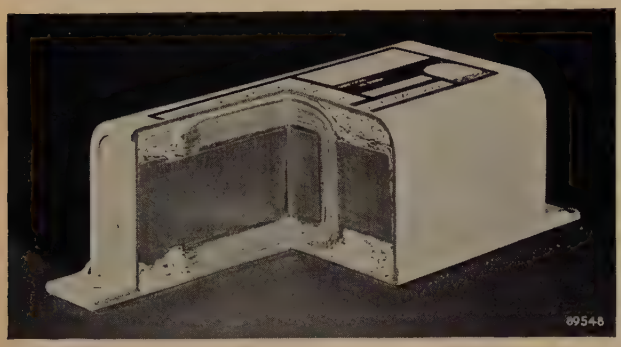

Fig. 2. Section of a ballast with a filling of dimpled aluminium foil.

quantity of aluminium, thermal conduction occurs via a large number of contact points: as a result the heat removal is just as efficient as in the case of complete filling with the best asphalt filler. Moreover, the crumpled aluminium foil is an effective remedy for rustle (the fairly high-pitched sound caused by free mechanical vibrations of choke or transformer cores, as described recently in this journal [2])).

Although very good results were obtained with aluminium foil, the search for better filling materials has continued, and has been directed notably towards electrical non-conductors which would obviate the need for applying insulation around the coils. Of the electrical non-conductor materials, the polyester group of resins soon attracted attention [3]). These resins can be cast and are excellent insulators; they are highly moisture-repellent and have a reasonable coefficient of thermal conduction (approx. 2×10^{-3} W cm^{-1} °C^{-1}). After casting, the resin hardens as a result of a chemical reaction and thereafter stays hard, even at the highest temperatures

[2]) E. W. van Heuven, The noise emission of ballasts for fluorescent lamps, Philips tech. Rev. **18**, 110-119, 1956/57, in particular pp. 118-119.

[3]) Miniaturizing with plastics, Brit. Plastics **24**, 302-307, 1951.

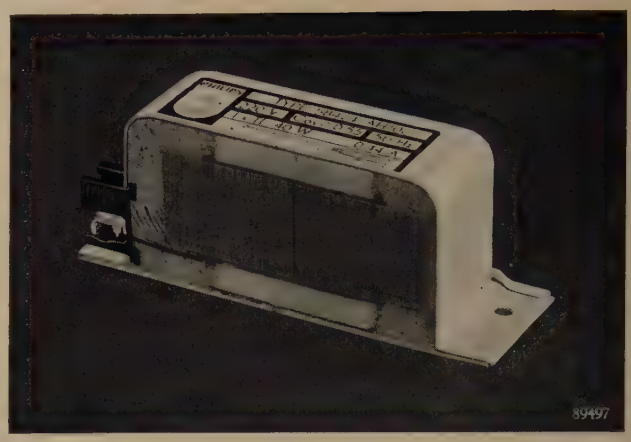

Fig. 3. Section of a ballast with a filling based on polyester resin.

that occur in ballasts. However, it shrinks quite considerably (by about 7%) and its price is high for a filling material. By admixing suitable substances these difficulties can be largely overcome, the shrinkage can be brought down to 1 - 2%, while at the same time the price is appreciably lowered and the thermal conduction is increased by a factor of 3 to 5. In its unhardened state the viscosity of the mixture can be made such that it penetrates well into narrow gaps; if necessary a gentle pressure can be applied to force it into such gaps. A few spaces will be left nevertheless, but they do not impede heat removal significantly and in practice therefore the ballast box can be considered to be completely filled (*fig. 3*).

The advantage to be gained with a filling mass based on polyester resin can best be illustrated by means of a few examples.

One of the most important ballasts is the inductive type for the 40 W fluorescent lamp and for 220 V mains. In the existing model with aluminium foil, the box is 122 mm long. In the new model the length has been reduced by 37% to 77 mm, the cross-section remaining the same. The choke coil itself has been reduced in length from 106 mm to 65 mm and has been somewhat enlarged in cross-section,

Table I. Data on 40 W fluorescent lamp ballasts, mains voltage 220 V, old and new forms (with aluminium foil and polyester filler, respectively).

	Aluminium foil	Polyester filler
Total length (mm)	150	105
Length of box (mm)	122	77
Weight (kg)	1.35	0.95
Losses (W)	9	9
Temperature rise (°C) *)	55	55

*) Measured with a 10% over-voltage and under the test conditions laid down by the International Commission on Rules for the Approval of Electrical Equipment.

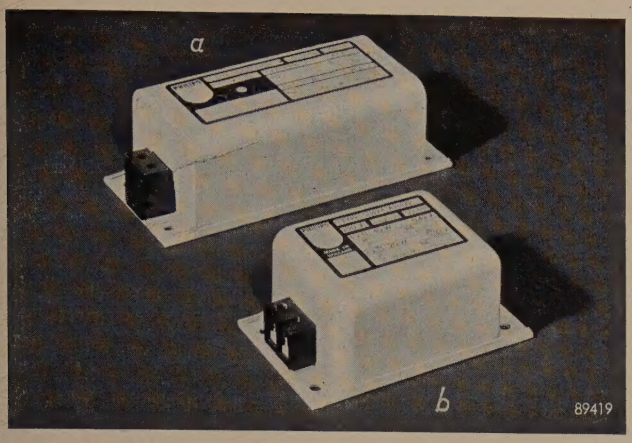

Fig. 4. Ballasts for 40 W fluorescent lamps, mains voltage 220 V. *a* is filled with aluminium foil, *b* with polyester resin.

this having been made possible by the good penetrating power of the filler. *Table I* gives some data on both models, which are shown in *fig. 4*.

The appreciable reduction in length has the additional advantage that the noise produced is considerably less (see the article cited in [2]): firstly, because the elastic movements of the choke or transformer core are smaller, owing to the greater rigidity of the shorter iron circuit, secondly, because the magnetostrictive movements are reduced (for a given magnetic induction they are proportional to the length) and thirdly, because the stray magnetic field is weaker, so that the forces acting on the steel housing are also less. The result of all this is that certain design changes are possible which were not feasible when using the aluminium foil filler, owing to the excessive hum that would be involved.

An example of such design changes is provided by the inductive ballast, again for 40 W fluorescent lamps, but this time for a mains voltage of 110 V. For ignition and stable burning the lamp requires a rated supply voltage of at least 200 V. Such a voltage can be obtained by means of an autotransformer. With the conventional design (i.e. autotransformer with only a very small flux leakage), a separate choke must be incorporated in series with the lamp, just as with a 220 V supply ballast. The conventional ballast thus comprises a transformer of about 100 VA and a choke of about 75 VA, both of which have a low hum level, with a filling of aluminium foil.

A better solution (being smaller and cheaper) is a leakage autotransformer. This is an autotransformer in which special provision is made for flux leakage between the two parts of the coil. A separate choke is then unnecessary if the leakage is given the correct value. *Fig. 5* shows a practical design [4]). Used with

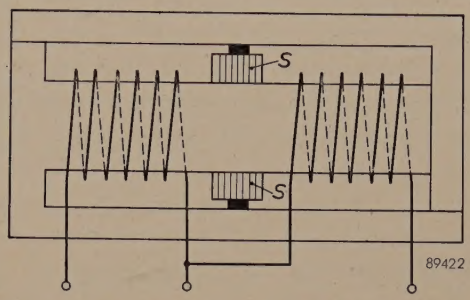

Fig. 5. Leakage autotransformer [4]). The laminated magnetic shunts *S* are driven to the required depth between the two parts of the coil to give the magnetic leakage the correct value; the shunts are then firmly wedged in place.

an aluminium-foil filling, such a leakage transformer with the normal cross-section would have to be about 170 mm long. With a transformer of this length the hum level cannot be suppressed to an acceptable value. Hitherto, therefore, there was no

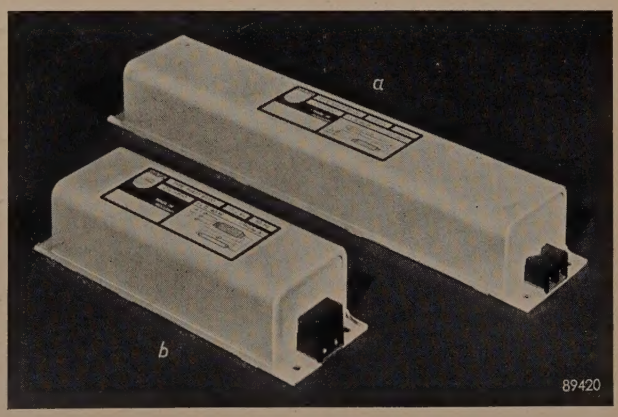

Fig. 6. Ballasts for 40 W fluorescent lamps, mains voltage 110 V. *a*) Separate transformer and choke. *b*) Leakage autotransformer, filling based on polyester resin.

alternative but to use the more costly solution: a separate transformer and choke. With polyester filler it has been possible to reduce the length so as to lower the hum level to a permissible value. Polyester filler therefore has "killed two birds with one stone" in this case. Some data on both models shown in *fig. 6* are given in *Table II*.

Th. HEHENKAMP.

Table II. Data on the ballasts for 40 W fluorescent lamps, mains voltage 110 V, old and new forms.

	Separate transformer and choke; aluminium foil filler	Leakage autotransformer; polyester filler
Total length (mm)	330	195
Length of box (mm)	302	167
Weight (kg)	3.1	1.85
Losses (W)	18	14
Temperature rise (°C) *)	65	55

*) Measured with a 10% over-voltage and under the test conditions laid down by the International Commission on Rules for the Approval of Electrical Equipment.

[4]) H. A. W. Klinkhamer, Philips tech. Rev. **1**, 342, 1936, fig. 7.

ABSTRACTS OF RECENT SCIENTIFIC PUBLICATIONS BY THE STAFF OF N.V. PHILIPS' GLOEILAMPENFABRIEKEN

Reprints of these papers not marked with an asterisk * can be obtained free of charge upon application to Philips Electrical Ltd., Century House, Shaftesbury Avenue, London W.C. 2.

2374*: H. J. G. Meyer: Some aspects of electron-lattice interaction in polar crystals (Dissertation, Amsterdam 1956).

This thesis gives a theoretical treatment of the phenomena which depend on the interaction of lattice vibrations with those electrons which make no contribution to the electrical conductivity. These electrons may be divided into two groups, viz. those which are bound to a defect in a perfect lattice and those which, together with a positive hole in the filled band, are bound to a mobile exiton (Parts I and II respectively of this dissertation). In Part I a survey is given of the effects of lattice vibrations on the transitions of lattice defect electrons — both transitions accompanied by radiation and those which occur without radiation. It is shown — as also in Part II — that all lattice vibrations which interact with electrons have the same frequency. In Part II the effect of the (constant frequency) lattice vibrations on the states of exitons is investigated, on the basis of an "effective mass approximation". The content of this part is substantially that of an earlier publication by the author (see these Abstracts No. 2353).

2375: K. H. Klaassens and C. J. Schoot: The reaction between silver phosphate and substituted phenoxyacetyl chlorides (Rec. trav. chim. Pays-Bas **75**, 265-270, 1956).

The reaction between silver phosphate and a number of substituted phenoxyacetyl chlorides is described. In all cases liberation of carbon monoxide is observed. After reaction, it is possible in some cases to isolate a substance with the formula $R\text{-}O\text{-}CH_2\text{-}O\text{-}CO\text{-}CH_2\text{-}O\text{-}R$, where R represents a substituted phenyl group. The remaining compounds form resins of the phenol-formaldehyde type, but under certain circumstances it is possible to identify an o-hydroxybenzyl alcohol. A possible mechanism for the reaction is discussed.

2376: C. J. Schoot and K. H. Klaassens: Plant growth activity and chemical structure (Rec. trav. chim. Pays-Bas **75**, 271-278, 1956).

A hypothesis relating to chemical structure and plant growth activity is formulated. The views of Hansch and Muir, Smith and Wain and Leaper and Bishop are correlated using as a basis the reaction between Ag_3PO_4 and phenoxyacetyl chlorides described in a previous article. The aryloxyacetic acids, the arylacetic acids and the arylcarboxylic acids are classified in the same scheme. Some indication is given as to the influence of the substituents in the phenoxyacetic acids. The rule of Leaper and Bishop is generalized.

2377: J. de Jonge and R. Dijkstra: Some photochemical properties of alkali salts of aryldiazosulphonic acids (Rec. trav. chim. Pays-Bas **75**, 290-300, 1956).

The structure of the labile form of an aryldiazosulphonate and the precise result of exposing a stable diazosulphonate to actinic light is considered to be still uncertain. From experiments on the action of light it can be concluded that a stable diazosulphonate is transformed into a product which is in solution at least partly, but possibly completely dissociated into diazonium ions and sulphite ions. For a number of diazosulphonates the quantum yield for the photochemical reaction has been determined.

2378: E. G. Dorgelo: Ueber die Technologie von Magnetrons und Klystrons (Vakuum-Technik **4**, 166-176, 1956).

After a short comparison of convential valves (triodes, tetrodes) with magnetrons and klystrons from the point of view of their application in pulse radar, a description is given of the construction of a few typical valve types. The main part of the article deals with general technological problems in the construction of magnetrons and klystrons. Special attention is paid to the cathode problem. It is the intention of the author to go deeper into the detail questions of manufacture in a second article.

2379: J. Bloem and F. A. Kröger: The p-T-x phase diagram of the lead-sulphur system (Z. phys. Chemie, Frankfurt a.M. **7**, 1-14, 1956).

The phase diagrams (p-T, p-x and T-x) of the Pb-S system, with special reference to the composition of the solid compound PbS, have been deter-

mined by electrical and chemical methods. The maximum melting point is found to lie at 1127 °C and corresponds to a solid PbS phase containing an excess of lead of 6×10^{18} atoms per cm^3 ($= 3\times10^{-4}$ atoms/mole). Anomalies in the shape of the curves for co-existing solids and liquids indicate the presence of short range order in the liquid at the composition PbS.

2380: J. Bloem and F. A. Kröger: The influence of heating in an inert gas atmosphere on the properties of a compound semiconductor, with special reference to PbS (Z. phys. Chemie, Frankfurt a.M. **7**, 15-26, 1956).

Compounds are stable with respect to heating in a stream of inert gas if the sum of the partial pressures of the components present in the gas phase in equilibrium with the solid has a minimum within the stability range of the solid compound. The solid then attains the composition at which it is in equilibrium with the vapour having the composition of the minimum. The same reasoning applies to heating in vacuo as long as the stationary pressure near the compound does not lie markedly below the minimum equilibrium pressure of the compound. The theory is checked for PbS, pure and doped with silver or bismuth, and good agreement with experiment is observed.

2381: J. Haantjes and K. Teer: Compatible colour television (Wireless Engr. **33**, 3-9 and 39-46, 1956).

In Part 1 a discussion of the requirements and possibilities for a compatible colour-television transmission system is given. A description of a transmission system using two sub-carriers for the additional colour information follows. In Part 2, the two sub-carrier (t.s.c.) system, described in Part 1, is compared with the American N.T.S.C. system. Particular attention is paid to the requirements to be met by the transmission channel, signal-to-noise conditions, cross-talk sub-carrier annoyance and receiver complexity.

2382: K. Rodenhuis: Life and reliability of radio tubes for professional equipment (T. Ned. Radiogenootschap **21**, 65-93, 1956).

Substantially the article which appeared in this Review, vol. 18, pp. 181-192, 1956.

2383: G. Diemer and P. Zalm: Voltage distribution inside electroluminescent ZnS crystals (Physica **22**, 561-562, 1956).

Brief note on a theoretical analysis of the voltage distribution in electroluminescing ZnS crystals, based on the hypothesis that local internal barriers give rise to high local field strengths.

2384: A. van Weel: Some remarks on the radio-frequency phase and amplitude characteristics of television receivers (J. Brit. Instn. Radio Engrs. **16**, 271-280, 1956.)

The influence on the picture of the steady-state characteristics of the radio-frequency part of a television receiver is considered especially for the frequencies close to the carrier frequency, the so-called Nyquist flank. It follows from numerical calculations that the shape of the amplitude characteristics of this Nyquist flank has but little influence on the picture quality. The performance of a receiver will be substantially the same in combination with a double-sideband transmitter as with a vestigial sideband transmitter, provided the latter has been compensated for its own phase errors. The performance of a vestigial sideband transmitter should be monitored with a phase-linear receiver, of which the exact shape of the Nyquist flank is not very critical.

2385: C. J. Heuvelman and A. van Weel: Group-delay measurements (Wireless Engr. **33**, 107-113, 1956).

A description is given of a simple group-delay meter which, in combination with any conventional wobbulator generator, gives the group-delay characteristic directly on an oscilloscope. An automatic-gain-control circuit, necessary to maintain a constant level at the output of the network under test, enables the tracing of the amplitude characteristic on a second oscilloscope at the same time. Calibration of amplitude and group-delay scales is possible for any oscilloscope used. A sensitivity of 1 millimicrosecond can be achieved. The frequency range is 20-45 Mc/s.

2386: J. S. C. Wessels: De Hill-reactie (Landbouwkundig Tijdschrift **68**, 647-655, 1956).

Survey article, in Dutch, concerning the Hill reaction; among the points discussed are methods for the study of the Hill reaction, comparison with photosynthesis, the role of the hydrogen donor and the nature of certain reduction processes.

2387*: F. A. Kröger: Inorganic crystal phosphors (Ergebn. exakt. Naturwiss. **29**, 61-144, 1956).

Comprehensive survey article on the present state of knowledge of inorganic crystal phosphors. Over 700 references are given.

2388: K. ter Haar and J. Bazen: The titration of nickel with EDTA at pH 2.8 (Anal. chim. Acta **14**, 409-413, 1956).

A method for determining nickel using EDTA is described. A small excess of EDTA is added, the pH adjusted to 2.7-2.9 and the solution back-titrated with thorium nitrate, against alizarin-S as indicator. Quantities of cobalt up to 10 mg do not interfere. In addition, an approximate determination of the complex-forming constant of Th-EDTA is described, based on the decrease in extinction of an Ni-EDTA solution to which Th^{+4} has been added.

2389: J. A. Haringx: Non-linearity of corrugated diaphragms (Appl. sci. Res. **A6**, 45-52, 1956).

Proceeding from the method of calculation for determining the rigidity of corrugated diaphragms given in a former paper, one is able to indiate what degree of non-linearity of the relations between load and deflection is to be expected for large deformations. By means of an example it is shown that the introduction of the corrugations into the flat plate, though unavoidably increasing the initial rigidity, involves an important gain in maximum deflection for the same degree of non-linearity.

2390: J. Bloem: p-n junctions in photosensitive PbS layers (Appl. sci. Res. **B6**, 92-100, 1956).

It has been possible to produce PbS layers containing sharp p-n junctions by partly coating a glass substrate with a trivalent metal and then precipitating a PbS layer from an aqueous solution. A photo-e.m.f. up to 300 mV was observed, corresponding to the value of the energy gap of about 0.3 eV. Some properties of these cells are discussed, attention being paid in particular to the influence of oxygen in the ambient gas.

2391: G. W. van Oosterhout: A rapid method for measuring coercive force and other ferromagnetic properties of very small samples (Appl. sci. Res. **B6**, 101-104, 1956).

A description is given of a method for the quantitative investigation of the permanent magnetic properties, especially the coercive force, of samples of about one milligram. The method is based essentially on the measurement of the alternating e.m.f., generated by letting the sample vibrate in a search coil, with a sensitive voltmeter. For the measurement of magnetic moments the instrument has to be calibrated. It is pointed out how this can be done. The time needed for a measurement is about two minutes.

2392: J. J. Opstelten, N. Warmoltz and J. J. Zaalberg van Zelst: A direct-reading double-sided micromanometer (Appl. sci. Res. **B6**, 129-136, 1956).

On each side of a thin diaphragm, separating two chambers, a condenser plate is mounted at a small distance. The two capacities thus formed are part of a bridge circuit which is fed by a high-frequency oscillator. An amplifier with a narrow bandwidth and a phase-dependent rectifier give a voltage which is fed back to the manometer. At one side of the diaphragm a pressure prevails, much lower than the one to be measured, at the other side the gas is admitted, the pressure of which is to be measured. The displacement of the membrane by the gas pressure is almost completely compensated electrostatically by the feedback voltage. By virtue of a differential way of feedback the reading is proportional to the pressure. The range is from 10^{-5}-0.5 mm of mercury pressure difference at any absolute value. The apparatus is made of chemically fairly resistant materials, and as its indication is independent of the nature of the gas, it can be used for almost every gas. The apparatus can also be used as a non-direct reading instrument, in which case the upper limit of the range is 1 mm of mercury.

Now available:

P. A. Neeteson: Analysis of bistable multivibrator operation. The Eccles-Jordan flip-flop circuit (Philips Technical Library, 82 pp., 34 figures).

The bistable multivibrator, invented by Eccles and Jordan in 1919, attracted little attention for many years, until it suddenly found wide application in pulse techniques. The book reported above (based on a doctoral thesis for the University of Delft) gives for the first time a detailed analysis of the mode of working, particularly of the phenomena which occur when the multivibrator is switching over. A practical result of this analysis has been the development of special valves for circuits of this type.

The twelve chapters of the book bear the following headings: 1. General introduction. 2. Survey of literature. 3. Introduction to the problem. 4. Opening or closing of switches in a network. 5 The static condition of the bistable multivibrator. 6. The dynamic condition. 7. The complete trigger cycle. 8. The trigger sensitivity. 9. The triggering speed. 10. Design considerations. 11. Variations of the fundamental circuit and way of triggering. 12. Conclusion. There follow five appendices with calculations.